RSC Chemical Biology

ROYAL SOCIETY OF CHEMISTRY

REVIEW

View Article Online
View Journal

Cite this: DOI: 10.1039/d6cb00005c

Recent progress in cGAS–STING agonist design and mechanisms of cancer immune modulation

Liao Wang,[a] Muhammad Nafees,[a] He Fei,*[a] Muhammad Hanif*[b] and Piaoping Yang*[a]

The cyclic GMP–AMP synthase (cGAS)–stimulator of interferon genes (STING) signalling pathway is a crucial modulator of innate immunity and an important target for next-generation cancer immunotherapy. Numerous cGAS–STING agonists have been developed and evaluated for their ability to promote anti-tumour immune responses. Cyclic dinucleotides (CDNs) are the most widely employed natural STING agonists; however, poor membrane permeability and enzymatic instability have motivated the development of non-CDN small-molecule agonists, including organic scaffolds and metal-based complexes with improved stability and tunable physicochemical properties. Additionally, nanomaterials that incorporate metal complexes with or without STING agonists have recently emerged as promising platforms for achieving robust therapeutic effects, facilitating targeted delivery, controlled release, and integration with other treatment modalities such as photodynamic therapy. This review offers a comprehensive examination of advancements over the past two years in the design and development of STING modulators, including organic scaffolds, metal-based complexes, and nanomaterials that encapsulate or tether metal-based drugs. It emphasises their chemical structures and the molecular mechanisms that facilitate STING activation and discusses significant challenges while delineating future research and therapeutic development directions.

Received 9th January 2026,
Accepted 1st May 2026

DOI: 10.1039/d6cb00005c

rsc.li/rsc-chembio

1. Introduction

Recent years have witnessed a significant expansion in our understanding of the immune mechanisms that protect against infection, malignancy, and tissue injury. The immune system comprises an integrated network of cells, tissues, and soluble mediators that sense perturbations to homeostasis and induce regulated responses to pathogens and cellular stress, while maintaining self-tolerance and limiting immunopathology.[1,2] Historically, it was widely assumed that immunological memory, particularly classical adaptive immunity, was confined to jawed vertebrates. This view was informed by the presence of specialised lymphocyte lineages (T and B cells) and antibody production, which together constitute core elements of the adaptive immune response.[3–5] Nonetheless, developments in cellular biology and genomics have elucidated that a type of immunological defense mechanism is widespread across living organisms, including jawless vertebrates and invertebrates.[6] Thus, the contemporary perspective holds that immunity is a basic biological function that has developed in various ways in all spheres of life, not only in complex animals.

Despite the immune system's critical role in warding off infections and maintaining homeostasis, diseases like cancer can develop when the immune system malfunctions or is misregulated.[7–9] In cancer, the immune system is both protective and destructive. The protective immune system operates as immune surveillance, which involves the ongoing monitoring of tissues by immune cells, specifically natural killer (NK) cells and cytotoxic T lymphocytes (CTLs), and the elimination of aberrant cells, particularly those harbouring tumourigenic mutations that may lead to tumour development.[10,11] However, this protective function can be undermined. In order to accomplish this, several tumours develop new ways to evade the immune system detection and elimination mechanisms. These approaches entail the production of immunological checkpoint proteins which attenuate T cell activity and foster immune tolerance towards the tumour.[12] Furthermore, tumours can enlist regulatory T cells (Tregs), myeloid-derived suppressor cells (MDSCs), and tumour-associated macrophages (TAMs) to create an immunosuppressive tumour microenvironment (TME). This milieu not only suppresses anti-tumour immunity but also facilitates tumour proliferation, angiogenesis, and metastasis.[13–15] Understanding these immune-cancer

[a] Key Laboratory of Superlight Materials and Surface Technology, Ministry of Education, College of Materials Science and Chemical Engineering, Harbin Engineering University, Harbin 150000, China. E-mail: hefei@hrbeu.edu.cn, yangpiaoping@hrbeu.edu.cn
[b] School of Chemical Sciences, University of Auckland, Auckland 1142, New Zealand. E-mail: m.hanif@auckland.ac.nz

interactions has transformed therapy approaches. Cancer immunotherapy seeks to rejuvenate the immune system and restore its ability to combat tumours.[16] Key approaches encompass immune checkpoint inhibitors (ICIs), cancer vaccines, adoptive cell treatments, and cGAS–STING agonists.[17–20] The convergence of these strategies highlights the growing impact of immunotherapy in reshaping cancer treatment, transition from traditional cytotoxic therapies to immune-based precision medicine, an advancement in which STING assumes a notably compelling role.

1.1 Understanding the cGAS–STING pathway: biological basis and operating principle

Intrinsic immune defence relies on the cGAS–STING pathway, which detects cytosolic double-stranded DNA (dsDNA) and triggers an immune response.[21,22] In healthy cells, DNA is contained within the nucleus and mitochondria. In the TME, atypical accumulation of DNA fragments in the cytosol can occur as a result of genomic instability, radiation-induced DNA damage, chemotherapy or mitochondrial rupture.[23] An enzyme called cyclic GMP-AMP synthase (cGAS) acts as a primary sensor to recognise dsDNA, which acts as a "danger signal" when it reaches the cytosol.[24,25] Direct binding of cGAS to dsDNA triggers a conformational shift within the enzyme complex, allowing it to carry out its function. When active, cGAS converts adenosine triphosphate (ATP) and guanosine triphosphate (GTP) into the production of a small signalling molecule known as 2′,3′-cyclic GMP-AMP (2′,3′-cGAMP). This molecule functions as a second messenger that binds to and activates STING.[26–28]

STING, an ~40 kDa multispanning transmembrane protein which is typically localized on the endoplasmic reticulum (ER) membrane, functions as an essential adaptor protein in this process.[29] In its dormant state, STING is inactive. When 2′,3′-cGAMP binds to STING, a conformational change reveals areas to facilitate STING's intracellular trafficking. As a result, STING departs from the ER to the Golgi apparatus through the ER–Golgi intermediate compartment. This translocation process involves genes associated with autophagy, like ATG9a and VPS34, which implies that autophagy is involved in STING regulation.[30,31] Here, STING serves as a platform to bring in subsequent signalling molecules, the most important of which is TANK-binding kinase 1 (TBK1).[32] Upon activation, TBK1 modifies a transcription factor known as Interferon Regulatory Factor 3 (IRF3). This modification enables IRF3 to translocate to the nucleus, where it functions as a switch, activating the genes that generate signalling molecules known as IFN-I (most notably IFN-β). Besides, STING also activates NF-κB (nuclear factor kappa-light-chain-enhancer of activated B cells) pathways, which lead to the production of proinflammatory cytokines (Fig. 1).[33,34]

Both NF-κB and IFN-I operate in a synergistic manner to enhance anti-tumour immunity by orchestrating robust immune responses and impacting tumour cells directly.[35] IFN-I augments dendritic cell (DC) maturation, boosts antigen-presenting cells (APCs), and activates CD8+ CTLs and NK cells, hence facilitating the immune system's capacity to effectively identify and eliminate tumour cells.[36] Moreover, IFN-I can directly induce apoptosis in tumour cells by activating pro-apoptotic genes such as TRAIL, Fas, and p53 and can

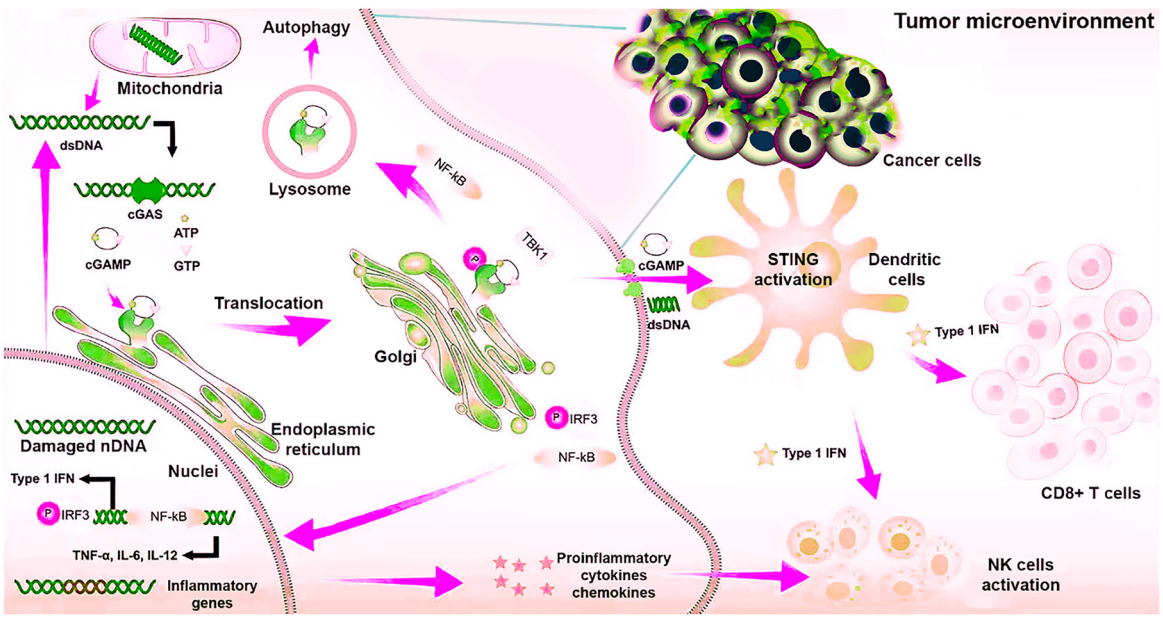

Fig. 1 Activation of the cGAS–STING pathway in cancer cells (created with Biorender and Adobe Photoshop). Cytosolic double-stranded DNA (dsDNA) from damaged nuclei and mitochondria of tumour cells activates cGAS, leading to the production of cyclic GMP–AMP (cGAMP), which then binds to and activates STING on the endoplasmic reticulum. Activated STING translocates to the Golgi apparatus, recruits TBK1, and causes the phosphorylation of IRF3. Nuclear IRF3 stimulates the expression of IFN-I and pro-inflammatory cytokines, hence augmenting dendritic cell activation and the recruitment of cytotoxic T cells and NK cells in the tumour microenvironment.

inhibit proliferation by causing cell cycle arrest through regulators like p21 and p27.[37–39] Concurrently, NF-κB facilitates anti-tumour immunity by stimulating pro-inflammatory cytokines, including TNF-α, IL-6, and IL-12, which augment immune cell infiltration, promote T cell priming, and establish an environment detrimental to tumour proliferation.[40,41] In addition, it enhances immune function by facilitating the activation of DCs, the polarisation of M1 macrophages, and Th1 (T helper type 1) responses, all of which contribute to the elimination of tumour cells.[42,43] Importantly, NF-κB-mediated cytokine signalling promotes immunogenic cell death (ICD), converting insufficiently immunogenic "cold" tumours into "hot" tumours marked by enhanced CD8+ T cell infiltration and phagocytic removal of dying cancer cells.[44] The synchronised activation of IFNs and NF-κB by STING generates a robust anti-tumour response, connecting innate detection with adaptive immune activation and direct tumour inhibition.

2. cGAS–STING agonist: classification and mechanism of action

Pharmacologically activating the cGAS–STING pathway has become a viable approach in tumour immunotherapy because of its crucial function in bridging innate and adaptive immunity. A wide variety of cGAS–STING agonists have been developed and assessed for their immunotherapeutic efficacy to leverage these effects. These agonists are generally categorized into various classes according to their molecular structures, therapeutic mechanisms, pharmacological characteristics, and translational relevance. As CDNs constitute the initial and most well-investigated category of STING agonists, their examination provides a crucial foundation for understanding subsequent advances. Consequently, we commence with CDNs prior to progressing to our main emphasis on small-molecule, metal-based complexes and nanomaterials.

2.1 Cyclic dinucleotides as cGAS–STING agonists

CDNs represent the most basic and thoroughly studied category of STING agonists that entered drug development. These compounds resemble 2′,3′-cGAMP that binds to and drives activation of STING.[45,46] Among the naturally occurring CDNs, 2′,3′-cGAMP is particularly significant due to its robust immunostimulatory capabilities (Fig. 2). 2′,3′-cGAMP is synthesised within human cells by cGAS upon the detection of dsDNA, activating the STING receptor and leading to the release of IFN-I and other pro-inflammatory cytokines. This activation puts 2′,3′-cGAMP as a crucial component in the development of cancer immunotherapies aimed at harnessing or enhancing the body's innate immune response against tumours.[47] Conversely, 3′,3′-cGAMP is a structurally analogous compound synthesised by specific bacterial species as a component of their signalling processes. While it may also initiate the STING pathway, its efficacy is markedly species-specific.[48] For example, 3′,3′-cGAMP has markedly reduced activity in human STING (hSTING) isoforms relative to its mammalian equivalent. Consequently, its immunostimulatory efficacy in human cells is constrained, diminishing its therapeutic promise in clinical applications, but it continues to serve as a significant

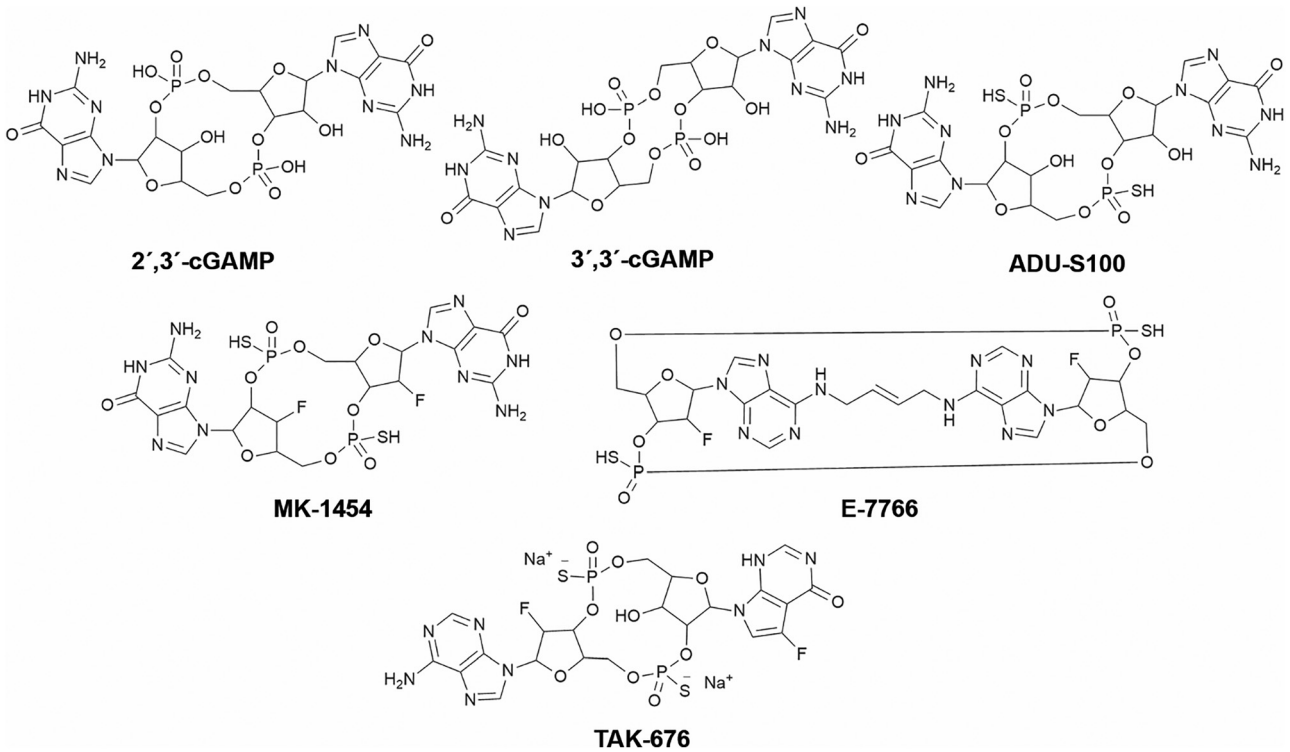

Fig. 2 Structures of natural and synthetic CDNs that induced STING-mediated anti-tumour immune response.

compound for investigating host–pathogen interactions and evolutionary differences in STING signalling.[49] Although 2′,3′-cGAMP and 3′,3′-cGAMP effectively activate STING and elicit strong immunological responses, their inadequate membrane permeability, vulnerability to enzymatic degradation, and restricted species-specific efficacy limit their practical applicability. To address these issues, researchers have synthesised STING agonists ADU-S100 (also referred to as MIW815), MK-1454, E-7766, and TAK-676 (Fig. 2). These compounds are structurally designed to improve stability, cellular absorption, and efficacy across various hSTING isoforms, rendering them more appropriate for therapeutic applications. ADU-S100, one of the first synthetic CDNs developed by Aduro/Novartis, is a phosphorothioate-modified CDN designed for intratumoural injection that elicits a strong IFN response, activates APCs, and enhances T cell infiltration within the TME. It has advanced to phase 1 clinical trials for metastatic triple-negative breast cancer (TNBC) and melanomas, utilised both as a monotherapy and in conjunction with ICIs such as anti-PD-1 antibodies (NCT02675439 and NCT03172936).[50] Nonetheless, despite its manageable toxicity and satisfactory response in the aforementioned clinical trials, the phase 2 clinical study of ADU-S100 for recurring or metastatic squamous cell carcinoma (NCT03937141) was discontinued due to insufficient anti-tumour activity.[51]

MK-1454, recently developed by Merck, mimics natural CDNs and is being examined in clinical trials for advanced solid tumours.[52] In clinics **MK-1454** was either administered alone or in conjunction with the anti-PD1 drug pembrolizumab (NCT03010176). In monotherapy, **MK-1454** did not elicit any response; however, in combination therapy with pembrolizumab, it exhibited partial responses of up to 24%, with a median reduction of 83% in the size of the target tumour.[53] Despite this promising efficacy, the safety profile of **MK-1454** presents challenges. The study demonstrated that treatment-related adverse events (TRAEs) occurred in 82–83% of patients in both monotherapy and combination therapy arms, with grade ≥ 3 events in 9–14%, and treatment discontinuation due to TRAEs in approximately 7% of patients in the combination arm. Notably, cytokine storm-like responses were observed upon dose escalation, characterized by marked increases in circulating pro-inflammatory cytokines, including IL-6 and IP-10, alongside robust induction of STING-responsive gene expression.[52] In a phase II clinical trial involving patients with recurrent head and neck squamous cell carcinoma (NCT04220866), the combination regimen attained a significantly elevated objective response rate, with 50% of patients demonstrating a noticeable therapeutic benefit, in contrast to merely 10% of those administered pembrolizumab alone. The median progression-free survival significantly increased from 1.5 months in the monotherapy group to 6.4 months with the combined therapy. Despite these promising efficacy results, the safety profile presented considerable challenges: 62.5% of patients undergoing the combination therapy encountered severe TRAEs, and 37.5% were compelled to terminate therapy prematurely due to toxicity.[54] Collectively, these clinical findings indicated that **MK-1454** effectively activates the STING pathway and promotes antitumor activity; however, it also induces cytokine storms associated with vascular leak syndrome, potentially contributing to its discontinuation and highlighting the limited therapeutic window of this systemically active STING agonist.

E7766, developed by Eisai, represents another unique class of synthetic STING modulators distinguished by improved antitumour responses in preclinical and clinical studies.[55,56] Unlike traditional CDNs, **E7766** possesses a non-nucleotide macrocyclic structure, enabling sustained STING activation while reducing systemic toxicity.[57,58] As of now, a business decision unrelated to safety has led to the withdrawal and termination of both clinical trials (NCT04144140 and NCT04109092) employing **E7766** for advanced solid tumours. **TAK-676** (also known as dazostinag) is another synthetic STING agonist that demonstrated significant immunomodulatory effects in preclinical conditions and permitted dose-dependent activation of immune cells and the generation of proinflammatory cytokines, thereby confirming its efficacy as a potent stimulator of innate anti-tumour immunity.[59] In clinical trials (NCT04420884), **TAK-676** administration triggered progressive activation of STING pathways, associated with increased expression of IFN-γ and IFN-γ-inducible protein 10 (IP-10).[60] In another clinical trial (NCT04541108), intratumoural microdosing of **TAK-676** either as monotherapy or in conjunction with standard chemotherapeutics induced IFN signalling, with combination therapy yielding superior local apoptotic responses compared to chemotherapy alone.[61] These preliminary results suggest a favourable and controllable safety profile of **TAK-676**; however, further data are needed to completely realise its potential as a therapeutic option for advanced solid tumours.

2.2 Synthetic small molecules as cGAS–STING agonists

Although CDN-based cGAS–STING agonists had strong immunostimulatory effects, their poor pharmacokinetics and restricted systemic potency have constrained their clinical application.[62] New approaches to cancer immunotherapy revolve around the design and development of organic scaffolds. These agonists have enhanced pharmacokinetic profiles and increased selectivity and potency towards STING by releasing more IFN-I, which subsequently augment T cell activation and induce tumour regression in several murine models. This section restricts its discussion to research published in the past two years. Readers interested in a comprehensive examination of prior studies are advised to refer to the cited literature.[58,63,64]

2.2.1 Canonical (direct) small-molecule STING agonists. Canonical small-molecule STING agonists are compounds that directly bind to the STING protein, inducing conformational changes, dimerization, and downstream signaling. These molecules mimic the natural CDN ligands, activating the cGAS–STING pathway to trigger IFN-I and other immune responses. The molecular structures of the pioneering organic STING agonists are shown in Fig. 3, illustrating the key scaffolds that enable direct STING binding and activation. Analysis of these

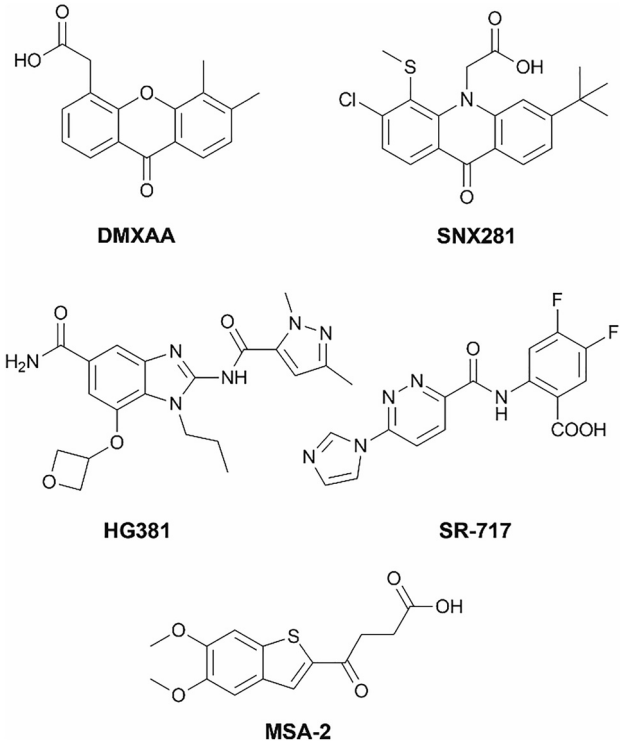

Fig. 3 Representative organic STING agonist scaffolds. **DMXAA** and **SNX281** were terminated in clinical trials, **HG381** (NCT04998422) is currently in clinical evaluation, and **MSA-2** and **SR-717** have not entered clinical trials.

early scaffolds highlights the importance of defined heteroaromatic cores, strategic polar functionalities, and conformational rigidity in enabling effective STING binding and downstream interferon signaling, thereby providing a structural blueprint for subsequent scaffold optimization.

Within the first generation of compounds, 5,6-dimethylxanthenone-4-acetic acid (DMXAA) was identified as one of the earliest synthetic small-molecule agonists of mSTING, exhibiting pronounced immunomodulatory activity.[65] Structural investigations revealed that **DMXAA** exclusively binds to mSTING, but not to hSTING, which explains its lack of efficacy in human clinical trials despite demonstrating significant antitumour effects in murine models.[66] Later, another research group further substantiated his mechanism by demonstrating that intratumoural injection of **DMXAA** in mice elicits strong $CD8^+$ T cell responses and facilitates substantial tumour regression in a STING-dependent manner.[67] These proof-of-concept investigations established **DMXAA** as a novel structure for the development of non-CDN small molecule STING agonists with enhanced efficacy against hSTING. The reverse optimization of compound **OS-1**, a structural counterpart of **DMXAA**, has recently been conducted, resulting in the synthesis of a series of new STING agonists.[68,69] Among them, **OS-2** was identified to be most potent and has been determined to be safe in experiments involving human peripheral blood mononuclear cells, as it does not independently trigger the production of cytokines (IFN-β, CXCL-10, and IL-6) but specifically enhances cGAMP-dependent STING activation (Fig. 4). By modifying STING oligomerization, **OS-2** augments innate immune responses while reducing systemic hyper-activation and off-target cytokine production. Furthermore, it exhibited significant anticancer efficacy against the B16.F10 murine melanoma model, which was further increased when used in combination with 2′,3′-cGAMP or the PD-L1 antibody. Although **DMXAA** and **OS-1** were included primarily as reference molecules, a qualitative structure–activity relationship can be inferred from their comparison with the newly developed compound **OS-2**. **DMXAA** contains a xanthone scaffold with a C4-linked carboxyl moiety. Scaffold replacement with an acridone core in **OS-1**, achieved through oxygen-to-nitrogen substitution, removal of the carboxyl group, and introduction of a C2-methoxy group while retaining the 5,6-dimethyl pattern, established the first broad-spectrum human- and murine-STING-active scaffold. Further optimization of the acridone core in **OS-2**, including the incorporation of an *N*-ethyl acetate substituent and fine-tuning of methyl and methoxy groups, generated a selective STING synergist with tumor microenvironment-restricted activity. Collectively, these compounds illustrate a scaffold-driven structure–function progression from a murine-specific agonist to a broad-spectrum activator and finally to a context-dependent synergist, highlighting the impact of scaffold choice and targeted substitutions on STING modulation.

Recently, Sun *et al.* used **DMXAA** as the initial reference scaffold to develop a library of 26 tricyclic derivatives in which the overall tricyclic topology was retained while key structural elements were systematically modified.[70] These modifications included replacement of the xanthone core with sulfur-containing tricyclic isosteres to modulate electronic properties, as well as introduction of methoxy substituents at selected positions to fine-tune electron density, lipophilicity, and steric profile. In addition, an alkyl chain linker was introduced to extend polar functionality beyond the rigid tricyclic core and enable additional intermolecular interactions. Screening of this tricyclic series identified **OS-3** as the most active compound, capable of activating both mSTING and hSTING (Fig. 4). While **OS-3** was derived from **DMXAA** at the design stage, extensive scaffold modification resulted in a structure that is chemically closer to **MSA-2** (a first-generation cell permeable STING agonist appropriate for oral administration) than to DMXAA.[71,72] This evolution reflects a shift from a xanthone-based framework toward a sulfur-containing tricyclic architecture optimized for STING activation. In **OS-3**, the presence of a carboxyl group may reduce cellular permeability, potentially limiting its anticancer efficacy *in vivo*; therefore, the authors transformed **OS-3** into a series of ester prodrugs. Among them, the methyl ester derivative, **OS-4**, was recognized as the most promising candidate (Fig. 4). **OS-4** activated mSTING in THP1 cells (EC_{50} = 9 μM) and was significantly more potent when compared with DMXAA (EC_{50} = 23 μM). Moreover, it significantly increased IFN-β production and improved STING, IRF3, and TBK1 phosphorylation, indicating strong STING pathway activation. In addition, **OS-4** had a 5.9-fold greater membrane permeability compared to **OS-3**, indicating enhanced cellular

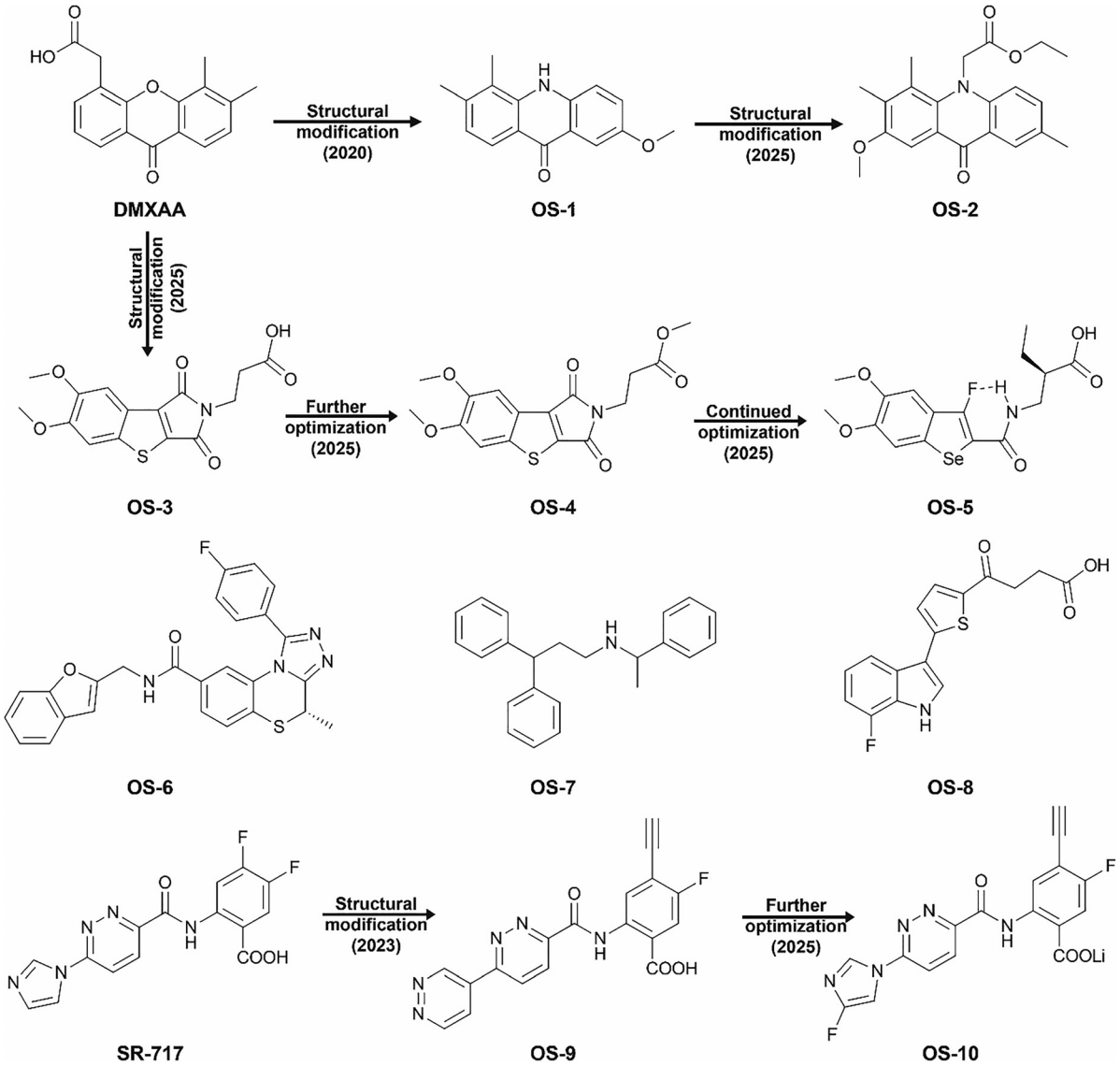

Fig. 4 Chemical structures of **DMXAA** and **SR-717**, and recently developed small organic scaffolds (OS) that directly bind to STING for anti-tumour immunotherapy.

absorption and tissue distribution. In an immunosuppressive pancreatic cancer model, **OS-4** in conjunction with anti-PD-1 significantly inhibited tumour development, resulting in 75% tumour growth inhibition (TGI) *via* subcutaneous administration (50 mg kg^{-1}) and 65% *via* oral administration (60 mg kg^{-1}), with negligible toxicity. Following this, the same research group developed another class of STING agonists by integrating an intramolecular hydrogen bond to mimic the rigid tricyclic conformation of **OS-4**, replacing sulfur with selenium and introducing an ethyl hydrophobic group at the α-position of the side chain.[73] Of the synthesized compounds, **OS-5** proved to be the most promising contender, exhibiting significant potency in activating the STING pathway (Fig. 4). **OS-5** facilitated significant phosphorylation of STING and its downstream effector IRF3, hence augmenting the synthesis and release of IFN-I, especially IFN-β. Furthermore, the oral administration of **OS-5** (60 mg kg^{-1}) exhibited substantial anticancer efficacy in the MC38 colon carcinoma model, leading to complete tumour regression and extended survival benefits. Interestingly, its therapeutic efficacy surpassed that of **MSA-2**, underscoring **OS-5** as a sophisticated next-generation oral STING agonist with considerable translational potential.

Surya *et al.* posited that the *N*-benzyl substitution would be more effectively aligned with the bioactive conformation by rigidifying the urea-based core and eliminating one benzylic carbon from their previous heterobicyclic STING modulators.[74–76] Based on these structural insights, they synthesized a series of tricyclic compounds as potential STING agonists.[77] Following a comprehensive structure–activity relationship (SAR) investigation, **OS-6** was identified as a lead candidate, demonstrating significant activation of key hSTING variants while exhibiting no activity against mSTING (Fig. 4).

Moreover, **OS-6** significantly induced the release of pro-inflammatory cytokines. Intratumoural administration of **OS-6** in hSTING knock-in mice bearing MCA205 fibrosarcoma tumours produced marked TGI (72%). Recently, Zhao *et al.* discovered **OS-7**, a small molecule with noteworthy effects on the STING pathway, target interactions, and anti-tumour immune activity (Fig. 4).[78] Genomic transcriptomic analysis revealed that **OS-7** treatment enriched interferon response and IL-6-JAK-STAT3 signalling pathways. By employing STING deficient cell lines, the authors found that **OS-7** activates TBK1-IRF3 in a STING dependent manner. In murine models, intratumoral injection of **OS-7** (300 μg per mouse) greatly reduced tumour growth by promoting immune cell infiltration and showed potent efficacy against refractory cold tumours (MC38, CT26, and B16F10). Meanwhile, intraperitoneal administration at doses of 5, 10, or 20 mg kg^{-1} every two days inhibited tumor growth in a dose-dependent manner.

Xie *et al.* recently developed a STING agonist, **OS-8**, and elucidated its mechanism of action (Fig. 4).[79] Crystal structure revealed that **OS-8** binds and activates both hSTING and mSTING. Its side chain penetrates deeper into the hSTING, which results in higher activity than that of the nucleotide-based STING agonist **ADU-S100**. Further mechanistic studies demonstrated that **OS-8** produces dose- and time-dependent activation of TBK1 and IRF3, enhancing anticancer cytokines (IFN-β, IL-2, IL-12, and IP-10), inflammatory mediators (TNF-α, IL-1β, IL-6), immunosuppressive IL-10, as well as chemokines and growth factors connected to immune activation and tissue repair. Furthermore, in syngeneic tumour models, **OS-8** exhibited substantial efficacy against melanoma, kidney, colon, and breast cancers, an effect abolished in STING-KO mice, exhibiting STING reliance.

SR717, alongside **DMXAA** and **MSA-2**, represents one of the early non-nucleotide STING agonists that stimulated interest in the design of structurally related analogues. Building on this scaffold, Zhang *et al.* explored a series of bipyridazine derivatives and identified compound **OS-9** (Fig. 4) as a particularly potent analogue with improved pharmacological properties relative to **SR717**.[80,81] Using the cocrystal structure of **SR717** bound to STING as a structural reference, the authors proposed a binding model for **OS-9**. Closer inspection of the binding model further revealed a compact, unoccupied region surrounding the pyridazine ring, indicating an opportunity for structural elaboration. This observation guided subsequent SAR optimization. In a later study, the pyridazine ring was replaced with an imidazole core, a modification that both preserved the essential water-mediated hydrogen-bond network and enabled the introduction of additional substituents into the previously unused pocket space. This rational scaffold modification ultimately led to the discovery of **OS-10**, a highly potent STING agonist with remarkable binding affinities to various hSTING variants and mSTING (Fig. 4).[82] **OS-10** exhibited significant cellular activity as compared to both **SR-717** and **OS-9**. Western blot analysis revealed that in comparison with **SR-717**, **OS-10** promoted a concentration-dependent phosphorylation of STING and its downstream effectors TBK1, IRF3, and p65 in THP1 cells. The RT-qPCR study also demonstrated that **OS-10** significantly upregulated the mRNA expression of STING-responsive genes IFNB1 and IL6 in a dose-dependent manner, thereby further validating its potential to activate the STING pathway. Moreover, **OS-10** exhibited markedly improved pharmacokinetic properties compared to **SR-717**, including an extended half-life (7.65 h *vs.* 1.8 h), reduced clearance (11.2 *vs.* 123 mL min^{-1} kg^{-1}), and greatly enhanced plasma exposure. **OS-10** achieved marked TGI (74.45%) when intravenously administered (10 mg kg^{-1}) in the B16.F10 xenograft mouse model. In addition, **OS-10** exhibited a significantly stronger inhibitory effect on the development of lung nodules linked to tumour metastasis. It also augments the infiltration of immune cells within the TME, specifically elevating the number of CTLs in comparison to the control and **SR-717** groups.

2.2.2 Nonclassical small-molecule STING agonists. In contrast to canonical STING agonists, nonclassical small-molecule STING agonists activate STING signaling through DNA damage-associated mechanisms rather than direct binding to the STING protein. By inducing genomic instability, DNA strand breaks, replication stress, or G-quadruplex stabilization, these molecules promote the accumulation of cytosolic nuclear or mitochondrial DNA, thereby triggering cGAS-dependent DNA sensing. This upstream activation ultimately converges on STING signaling and downstream interferon responses. This subsection summarizes representative small molecules that exemplify this indirect and mechanistically distinct mode of STING pathway activation.

Perylenediimide derivatives have become attractive biomedical agents because of their electron-deficient core, which promotes the production of endogenous reactive oxygen species (ROS) by enabling radical anion generation in hypoxic tumours. Furthermore, their amenable sites facilitate the substitution of sulfonic acid to enhance the stability of CDNs.[83–85] Leveraging these features, Ying, Huang and co-workers synthesized a sulfonated perylene termed as **OS-11** (Fig. 5).[86] The compound elicits ROS, resulting in the destruction of mitochondrial DNA (mtDNA) and nuclear DNA (nDNA), hence facilitating the synthesis of 2', 3'-cGAMP. Furthermore, **OS-11** attained a half-life of 8.22 hours, providing sufficient duration to effectively inhibit the enzymatic hydrolysis of 2', 3'-cGAMP. Upon administration, **OS-11** activated the cGAS–STING signalling pathway, demonstrated by a 13.7% augmentation in helper T cells and a 2.5- to 2.6-fold elevation in CTLs, consequently exhibiting substantial anticancer activity in tumour-xenografted mice.

G-quadruplexes (G4s) are non-canonical nucleic acid configurations driven by guanine-rich DNA or RNA sequences *via* stacked G-tetrads through Hoogsteen hydrogen bonds.[87,88] In addition to nDNA, they also found in mtDNA, where the lack of protective histones facilitates their development.[89] By disrupting replication machinery, mtDNA G4s undermine mitochondrial genome stability, a weakness that can be leveraged for cancer therapy, as G4 stabilization impedes critical pathways in tumour progression.[90,91] In this effort, Wang *et al.* developed a small library of triphenylamine-based compounds through the

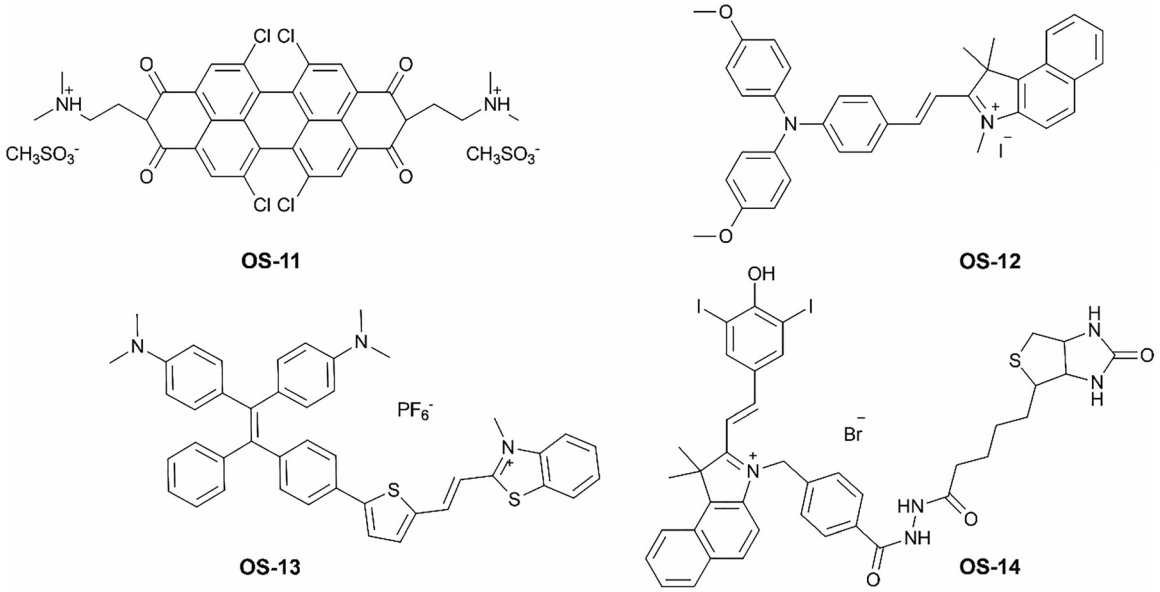

Fig. 5 Nonclassical small molecule STING agonists that activate STING through a DNA damage-associated mechanism.

Knoevenagel condensation reaction. These compounds exhibited the ability to target mtDNA G-quadruplexes to combat drug resistance and improve anti-tumour immunity in TNBC.[92] Among the synthesized compounds, **OS-12** demonstrated the highest potency with significant therapeutic activity (IC_{50} = 1.8 ± 0.1 μM) against TNBC cells (Fig. 5). Subsequent studies demonstrated that **OS-12** preferentially accumulates in the mitochondria, induces mtDNA damage, disrupts mitochondrial membrane potential (MMP), and generates ROS. Damaged mtDNA triggered the cGAS–STING pathway, which led to DC maturation and cytokine upregulation (IFN-β, ISG54, IL-6, and TNF-α). Moreover, **OS-12** (2.5 mg kg^{-1}) inhibited tumour growth and metastasis in 4T1 cell-bearing mice through the modulation of the TME, including macrophage remodelling and T cell activation. Interestingly, **OS-12** has become the first reported compound that activates the cGAS–STING immunomodulatory pathway by specifically targeting mtDNA G4s.

Phototherapy utilizes photosensitizers (PSs) to induce cellular death by the generation of ROS or heat.[93,94] Driven by these benefits, recent research focuses on constructing organelle-targeted aggregation-induced emission (AIE) photosensitizers that are suitable for hypoxic conditions and capable of generating ROS to alleviate tumour hypoxia, facilitate DNA release, and augment cGAS–STING activation.[95–97] Zhao *et al.* developed cationic AIE photosensitizers (**OS-13**, Fig. 5) that promote mitochondria-to-nucleus translocation for targeted cancer therapy by stimulating the cGAS–STING signalling pathway.[98] The PS was developed by integrating *N*,*N*-dimethyl-substituted tetraphenylethene (TPE) and the thiophene donor with benzothiazolium or the thiazolium acceptor, yielding NIR-II emission at 1080 nm and type I ROS generation. The twisted TPE unit equilibrates radiative and non-radiative decay, enabling a photothermal conversion efficiency of 63.6%. Upon exposure to 635 nm laser irradiation, **OS-13** caused mitochondrial damage, nuclear translocation, and the release of mitochondrial and nuclear DNA fragments. This leads to increased amounts of phosphorylated STING in cells, activation of several STING-related proteins, and the induction of ICD through the release of DAMPs. Moreover, following the encapsulation in DSPE-PEG nanoparticles (NPs) and upon intravenous administration in CT26 xenograft BALB/c mice, **OS-13** exhibited rapid tissue penetration (<6 h) and high-contrast NIR-II FLI/PTI-guided phototoxicity, leading to efficient solid tumour ablation.

Recently, Zeng *et al.* synthesised a multifunctional PS (**OS-14**, Fig. 5) *via* a biotin targeted-group-assisted methodology.[99] **OS-14** was engineered to interfere with the pyroptosis and stimulate the cGAS–STING pathways, thus augmenting both innate and adaptive anti-tumour immunity. Cellular studies revealed that **OS-14** selectively accumulated in lysosomes through energy-dependent endocytosis and when exposed to light (580 nm, 40 mW cm^{-2}, 5 min), exhibited significant phototoxicity across all breast cancer cell lines. **OS-14** damages mitochondria, releases mtDNA, and activates the cGAS–STING pathway by upregulating the phosphorylation of critical proteins, including IRF3, TBK1, and STING. Moreover, **OS-14** treatment induces substantial morphological changes in cancer cells, characterised by balloon-like membrane growth instead of the conventional apoptotic cell shrinkage and membrane blubbing, confirming a pyroptosis-like mode of cell death. In addition, confocal microscopic images showed that light activated **OS-14** treatment caused a cytoplasmic Ca^{2+} surge that accumulated in mitochondria, resulting in Ca^{2+} overload and subsequent mitochondrial dysfunction. In MCF-7 tumour-bearing nude mice, the intratumoural administration of **OS-14** led to a complete reduction in tumour growth, accompanied by negligible changes in murine body weight, indicating significant anticancer efficacy and low systemic toxicity.

2.3 Metal-based compounds as cGAS–STING activators

In addition to CDNs and organic scaffolds, recent focus has turned to metal-based compounds as a novel category of cGAS–STING pathway activator. The unique chemistry of metal centres, which includes various coordination geometries, variable oxidation states, and the ability to establish interactions unattainable by just organic molecules, offers avenues to alter pathways innovatively.[100,101] Moreover, metal-based compounds have adjustable physicochemical characteristics, such as stability, solubility, and cellular absorption, which can be utilized to enhance immunostimulatory efficacy.[102–105] These attributes render these compounds as a compelling foundation for the systematic development of next-generation cGAS–STING activators. This section addresses the metal-based compounds developed within the past two years that activate the cGAS–STING pathway and trigger the anti-tumour immune response.

Conventional platinum drugs primarily target nDNA, adversely affecting both healthy and malignant cells, whereas newer platinum complexes act on organelles, proteins, signaling pathways, or mtDNA to induce cytotoxicity.[106–108] Guo, Wang, and co-workers developed a monofunctional trinuclear platinum complex, **MC-1** (Fig. 6A), that forms DNA adducts and exhibits strong cytotoxicity against lung carcinoma cells.[109] Their recent study revealed that **MC-1** selectively impairs mtDNA in A549 cells, while exerting little effect on HK-2 cells, indicating mutation-dependent targeting.[110] Upon mechanistic investigations, they found a robust binding of **MC-1** to DNA, mediated by long-range crosslinks and DNA condensation, which is attributed to its trident structure and high positive charge (Fig. 6B and C). Confocal microscopic images demonstrated that mitochondrial fluorescence nearly disappeared while nuclear fluorescence remained intact, further confirming that **MC-1** selectively damages mtDNA (Fig. 6D). Western blot analysis revealed the activation of the cGAS–STING pathway, displaying increased levels of cGAS, STING, p-TBK1, IRF3, p-IRF3, and IFN-β. In contrast, CDDP induces a

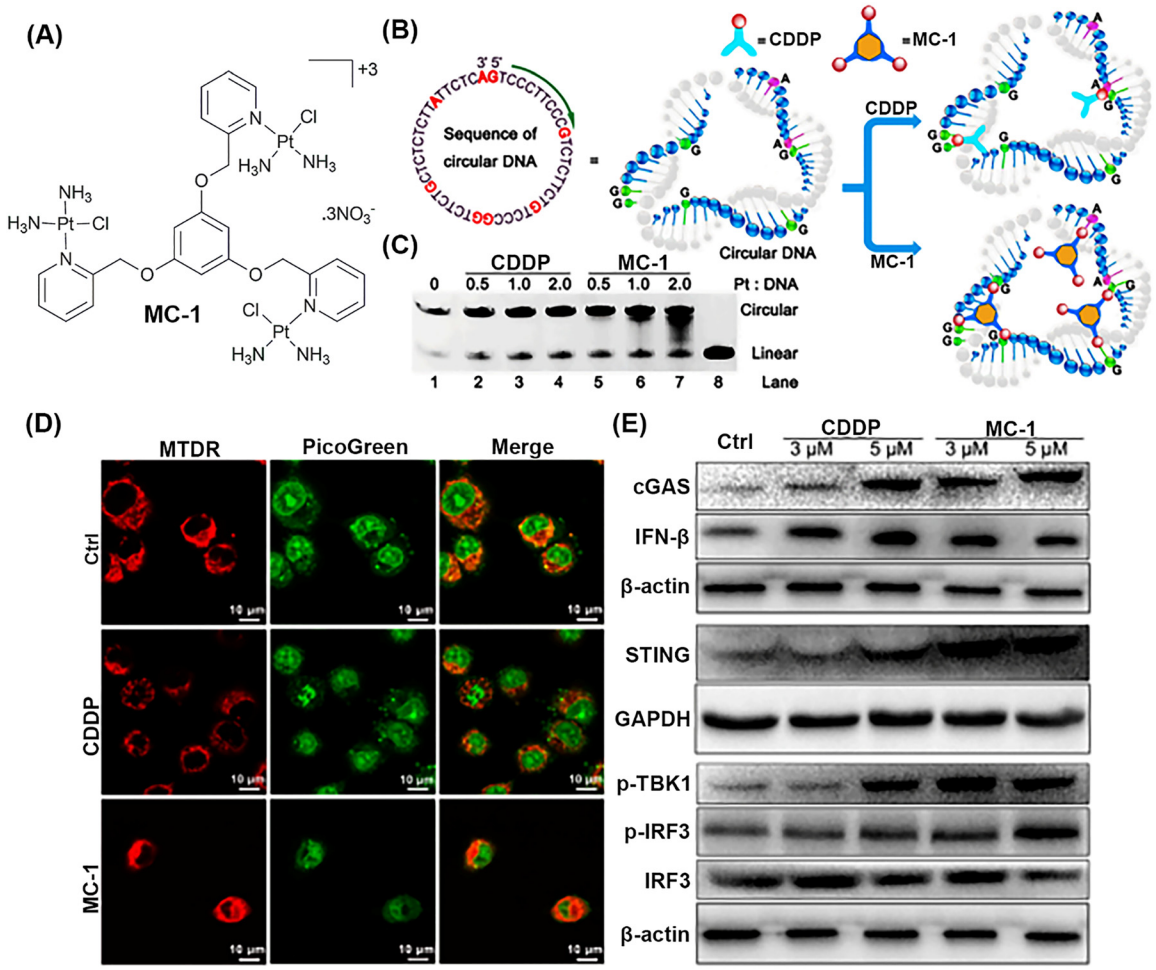

Fig. 6 Chemical structure of **MC-1** (A). Proposed binding interactions of CDDP and **MC-1** with a circular single-stranded DNA model containing sparsely distributed guanine and adenine residues and polyacrylamide gel electrophoresis patterns of circular DNA after treatment with different concentrations of cisplatin and **MC-1** (B) and (C). Confocal microscopic images illustrating the release of mtDNA upon respective treatment (D). Expression of cGAS, STING, IFN-β, p-TBK1, IRF3, p-IRF3, BAK, and BAX proteins after treatment with CDDP and **MC-1** (E). Adapted and modified with permission from ref. 110. Copyright 2025 American Chemical Society.

weaker pathway activation, primarily through nDNA damage, highlighting **MC-1** as a more potent cGAS–STING activator (Fig. 6E).

Combination therapy has generated interest among oncologists and bioinorganic chemists due to the synergistic effects produced by the individual drugs against tumours.[111] For example, a nanosystem that simultaneously administers the chemotherapeutic drug SN38 and the STING agonist **DMXAA** has been documented to provoke a robust STING-mediated anti-tumour immune response in various murine models.[112] But single-molecule multitargeted drugs are preferred over combination therapy because they are easier to use, have a lower chance of interactions, have predictable pharmacology, and improved safety and efficacy.[113,114] With this in mind, Guo *et al.* constructed two Pt^{IV} conjugates (**MC-2** and **MC-3**, Fig. 7) by tethering STING agonist **MSA-2** at the axial positions of oxoplatin.[115] Among them, **MC-2** showed potent cytotoxicity across multiple cancer cell lines and robust anti-tumour activity in C57BL/6 Pan02 tumours. Mechanistic studies revealed that **MC-2** enters cancer cells *via* energy-dependent transport, is reduced to cisplatin for DNA binding, and uniquely upregulates innate immunity and metabolic genes, including pyrimidine metabolism (rare among Pt drugs).

MC-2 stimulated the STING pathway in bone-marrow DCs and induced the release of immunogenic factors (IFN-β and IL-6) from cancer cells. Flow cytometry and single-cell RNA-seq revealed enhanced NK-cell infiltration and activation of T cells and DCs, which confirmed a strong anti-tumour immune response. The authors concluded that integrating a DNA-damaging agent and a STING agonist within a single molecule amplified STING activation and fully engaged both innate and adaptive immunity, thereby supporting its promise as a future cancer immunotherapy, potentially in combination with anti-PD-1/PD-L1 therapy.

Yang *et al.* constructed a triple-action Pt^{IV} prodrug (**MC-4**, Fig. 7) by conjugating the STING agonist **MSA-2** and a carbonic anhydrase IX (CAIX)-targeting moiety to the axial positions of oxoplatin.[116] HPLC analysis confirmed that **MC-4** is reduced to release cDDP together with its axial payloads (**MSA-2** and **CAIX**). Under hypoxic conditions, **MC-4** showed 2- to 7-fold increase in toxicity against several cancer cell lines. Mechanistic studies confirmed that the complex caused significant DNA damage and induced apoptosis through the activation of PARP and caspase-3. Moreover, **MC-4** was selectively internalized by hypoxic colon cancer cells *via* CAIX-mediated endocytosis. The compound obstructed extracellular acidification and the spread of colon cancer cells by inhibiting HIF-1α-mediated CAIX expression. Furthermore, **MC-4** stimulated STING signalling, enhanced IRF3 phosphorylation and cytokine production in HT29, THP-1, and RAW264.7 cells. In CT-26 tumours, the complex exhibited enhanced efficacy, diminished toxicity, mitigated hypoxia, and remodelled the TME by augmenting the infiltration of NK cells and M1 macrophages while reducing M2 macrophages.

Acetaminophen is well-known to inhibit Sam50, a mitochondrial protein that connects the inner and outer membranes, resulting in membrane remodelling and the release of mtDNA.[117,118] In hepatocytes, this mtDNA release triggers the STING pathway, leading to the accumulation of inflammatory factors and liver damage.[119] Wei *et al.* tethered acetaminophen to the axial locations of oxaliplatin (Oxa) to form a dual-action Pt^{IV} complex (**MC-5**, Fig. 7).[120] **MC-5** exhibited ten-fold higher cytotoxicity in comparison with its parental complex and triggered the innate immune response and IFN-I pathway. It suppresses Sam50 protein production, allowing Bax proteins to form mitochondrial membrane holes and release more mtDNA. The complex induces mitochondrial oxidative stress increased NLRP3 inflammasome production, triggering caspase-1 maturation for GSDMD-mediated pyroptosis. Moreover, **MC-5** promotes DCs maturation, cytotoxic T cell infiltration, and anti-tumour immune factors, consequently promoting a ''cold'' to ''hot'' TME. In addition, **MC-5** shrinks lung nodules and improves the efficiency of ICI in tumour metastasis models.

Copper metabolism plays multiple roles in cancer progression.[121] It stimulates cellular proliferation, enhances oncogenic signalling, facilitates metastasis, promotes angiogenesis, and enables immune evasion (cuproplasia). Conversely, copper inhibits tumour growth by activating regulated cell death pathways including apoptosis, pyroptosis, necroptosis, ferroptosis, and autophagy, as well as by activating anti-tumour immunity.[122–124] As a nonapoptotic pathway, cuproptosis is characterized as a copper-dependent cell death resulting from copper binding to lipoylated tricarboxylic acid cycle enzymes, which induces protein aggregation, proteotoxic stress, and ultimately cell death.[125,126] Recently, the dipyridophenazine copper complex, Cu-DPPZ, has been modified with a phenyl group (Ph) and a pyridine cation group (Py^+) to obtain two structurally similar copper complexes (**MC-6** and **MC-7**, Fig. 7) for the purpose of examining the distinct immune signalling mechanisms elicited by copper-mediated cuproptosis or apoptosis.[127] Cellular investigations illustrated that **MC-7** preferentially targets mitochondria relative to **MC-6**, facilitates the release of cytochrome *C* from mitochondria, and induces substantial aggregation of dihydrolipoamide *S*-acetyltransferase for cuproptosis without triggering the apoptotic pathway. Moreover, in comparison to CDDP, **MC-7** induces a significantly more robust activation of various immune and inflammatory pathways, including the TNF signalling pathways, the herpes simplex virus 1 infection pathway, IL-17 signalling, and the cytosolic DNA-sensing pathway, indicating a more extensive immunomodulatory effect. Because cuproptosis causes mtDNA to become more abundant in the cytoplasm, the author discovered that **MC-7** increased the expression of p-IRF3 and p-STING proteins, which in turn caused the release of interferons. Furthermore, in bilateral 4T1 tumour models, **MC-7** markedly enhanced the maturation of DCs and demonstrated superior T cell activation and infiltration relative to **MC-6**. This implied that the activation of innate immunity by cuproptosis depended on mitochondrial targeting provided by carbon–nitrogen single-atom transmutation.

Benzo[*i*]dipyrido[3,2-*a*:2′,3′-*c*]phenazine (dppn) is a planar, extended polyaromatic ligand well-known for its strong DNA-intercalating ability. Its large, rigid π-conjugated system allows insertion between DNA base pairs, thereby stabilizing the DNA–ligand complex through π–π stacking interactions.[128] Mao, Tan, and colleagues had developed a highly luminous Rh^{III} complex

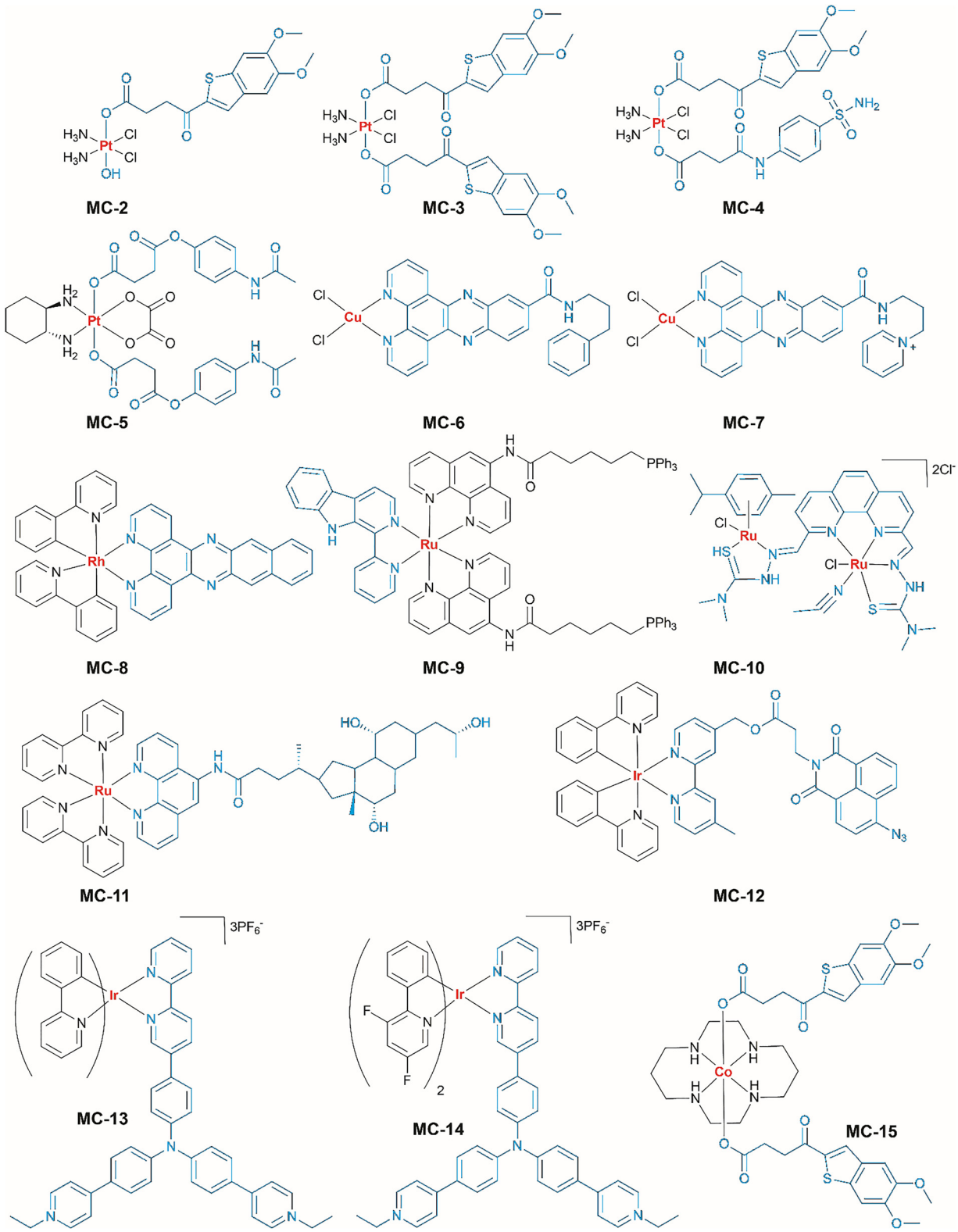

Fig. 7 Structures of recently developed metal-based compounds as STING agonists for anti-tumour immunotherapy.

by integrating the mtDNA intercalating ligand dppn (**MC-8**, Fig. 7). **MC-8** was designed to activate the STING signalling system, thereby augmenting anti-tumour immune responses for cancer immunotherapy.[129] Cellular studies demonstrated that **MC-8** inserted its biological action predominantly by targeting mitochondria, where it damaged mtDNA, significantly disrupting nucleotide anabolism and affecting the availability of essential metabolites involved in DNA methylation processes. RNA sequencing investigation revealed that **MC-8** therapy induced extensive changes in 5-methylcytosine (5mC) DNA modification patterns. This epigenetic remodelling served as a powerful immunogenic signal that activated the STING pathway, leading to significant IFN-I production. To enhance solubility and distribution, **MC-8** had been encapsulated within human heavy-chain ferritin (HFn) nanocages. *In vivo* findings indicated that the HFn-**MC-10** nanoconstruct significantly stimulated a robust anti-tumour immune response and inhibited both primary and distant tumours in Balb/C mice carrying U14 cancers.

The self-assembly of therapeutic compounds into nanoscale structures reduces toxicity, immunogenicity, and stability issues associated with synthetic carriers, while enhancing formulation and delivery efficiency.[130–132] Ling and colleagues synthesized a ruthenium complex in which two ancillary ligands bear triphenylphosphine-modified alkyl chains, while the core ligand is a bioactive derivative of the β-carboline alkaloid (**MC-9**, Fig. 7).[133] Owing to its ability to engage in numerous noncovalent intermolecular interactions, **MC-9** autonomously self-assembles into stable NPs with a uniform spherical morphology. Flow cytometry results revealed that light-activated **MC-9** induced 20-fold increase in cellular ROS levels and mitochondrial activities were considerably impaired. To directly investigate the ability of **MC-9** to trigger the cGAS–STING pathway, the authors first assessed the presence of cytoplasmic dsDNA. Confocal microscopy results demonstrated the appearance of large, intensely fluorescent mitochondrial nucleoids dispersing into the cytoplasm, confirming the presence of dsDNA. In addition, γH2AX, an indicator of DNA damage, was significantly upregulated. Consequent analysis revealed that **MC-9** driven PDT treatment markedly boosted the expression of cGAS and p-STING. In the 4T1 murine xenograft model, **MC-9** markedly suppresses the growth of both primary (58%) and distant (84%) tumours relative to the control groups, while no significant alteration in the weight of the mice was recorded, suggesting an absence of noticeable adverse effects.

Thiosemicarbazones represent a distinct class of anticancer agents, defined by a structure that includes one sulfur atom and two nitrogen atoms with lone pairs, which endows them with substantial metal-binding potential.[134,135] Considering this, a series of Ru^{II} 1,10-phenanthroline-2,9-diformaldehyde thiosemicarbazone complexes were synthesised, and their SAR was assessed.[136] Among the developed compounds, the arene binuclear Ru^{II} complex **MC-10** exhibited superior potency, significant cytotoxicity, and pronounced mitochondrial accumulation in tumour cells (Fig. 7). In order to enhance **MC-10** *in vivo* targeting and administration, an apoferitin-based nanodrug system (AFt) was developed. TEM revealed that **MC-10** AFt NPs exhibited a spherical morphology with a diameter of 11.6 nm. Following treatment with **MC-10**/**MC-10** AFt NPs, there was an elevation in cGAMP levels and a notable upregulation of p-STING, p-IRF3, and p-TBK1, but non-phosphorylated proteins remained unaltered. pSTING was also significantly upregulated in tumour tissues, while p-IRF3 was elevated and translocated into the nucleus, indicating that **MC-10**/**MC-10** AFt NPs stimulated the cGAS–STING pathway both *in vivo* and *in vitro*. Furthermore, the therapeutic efficacy of **MC-10** AFt NPs in mouse models surpassed that of **MC-10**, demonstrating a greater TGI (69.3% compared to 43.6%). They also exhibited enhanced antimetastatic efficacy, resulting in a reduced number and size of lung nodules compared to **MC-10**.

Impaired protein folding and dysregulated protein degradation in cancer cells lead to the accumulation of misfolded proteins in the ER. This disruption of ER proteostasis induces ER stress, subsequently activating the unfolded protein response to restore cellular homeostasis or trigger apoptosis.[137,138] In this context, cholic acid–conjugated prodrugs preferentially accumulate in the ER of cancer cells, exacerbating ER stress, disrupting MMP, and elevating ROS levels, thereby inducing both ICD and necrosis.[139,140] Recently, a cholic acid-modified Ru^{II} complex has been developed to combine effective photodynamic activity with selective ER delivery (**MC-11**, Fig. 7).[141] **MC-11** effectively produces singlet oxygen when exposed to light (450 nm) and demonstrates NIR-AIE phosphorescence for imaging. **MC-11** preferentially accumulates in the ER of MDA-MB-231 and 4T1 breast cancer cells, where light activation induces excessive ROS generation and significant ER stress. This stress significantly increases the STING signalling pathway, encompassing p-TBK1, p-STING, and p-IRF3, which induces Golgi stress, pyroptosis, and the secretion of anti-tumour proteins to trigger ICD. *In vivo* administration of **MC-11** (5 mg kg^{-1}) stimulated the adaptive anti-tumour immune response and significantly suppressed tumour proliferation in Balb/c mice carrying 4T1 tumours.

Hydrogen sulfide (H_2S) is recognised as a gaseous signalling molecule and a regulator of intracellular redox balance.[142,143] It enhances glutathione (GSH) levels by upregulating cystine/cysteine transporters, promoting precursor ingestion for GSH synthesis, and redistributing GSH to mitochondria to maintain redox balance and protect against oxidative stress.[144] Increased H_2S concentrations in tumours like colon adenocarcinoma and melanoma indicate a correlation between H_2S metabolism and tumour advancement.[145,146] This presents a therapeutic potential since H_2S-responsive theranostics can selectively utilize H_2S, disturb redox equilibrium, produce ROS, and diminish GSH to trigger ferroptosis, leveraging tumour-specific H_2S for targeted cancer treatment.[147] Building upon this understanding, an H_2S-responsive Ir^{III} complex containing an azide-substituted naphthalimide ligand has recently been synthesized as a ferroptosis inducer (**MC-12**, Fig. 7).[148] **MC-12** demonstrated the capability to distinguish tumours by variations in H_2S levels, preferentially illuminating H_2S-rich tumours and

enabling targeted cancer therapy through light exposure. Subcellular distribution studies demonstrated that **MC-12** primarily localizes in mitochondria, where it generates significant mtDNA damage, hence augmenting anticancer efficacy upon light irradiation. Moreover, **MC-12** induces significant ROS production and reduces intracellular GSH, hence facilitating ferroptosis *via* lipid peroxidation accumulation and the downregulation of GPX4, a crucial regulator of ferroptosis. In addition, **MC-12** treatment led to significant mtDNA damage which consequently activates the cGAS–STING pathway. RNA-seq analysis further revealed that **MC-12** mediated PDT treatment primarily modifies the expression of genes associated with ferroptosis, autophagy, and cancer immunology, underscoring its complex mechanism of anticancer activity.

Inducing a hybrid form of cell death that integrates pyroptosis and ferroptosis constitutes a viable approach for cancer treatment.[149] Pyroptosis induces significant inflammation and the secretion of DAMPs and cytokines, whereas ferroptosis promotes iron-dependent lipid peroxidation and oxidative stress.[150–153] Collectively, these pathways can synergistically boost immunogenic signals, improve tumour APCs, and elicit more robust innate and adaptive immune responses than either system independently, providing a potential strategy to counteract tumour immune evasion. Zheng *et al.* developed two Ir^{III} triphenylamine PSs with the capacity to simultaneously induce ferroptosis and pyroptosis for synergistic tumour immunotherapy (**MC-13** and **MC-14**, Fig. 7).[154] Cellular studies reveal that both complexes significantly disrupted the intracellular redox equilibrium, hence rendering tumour cells more susceptible to oxidative stress. Upon exposure to light (425 nm), **MC-13** and **MC-14** induced significant DNA damage and impaired the KEAP1 signalling pathway. Damaged DNA is expelled into the cytoplasm to activate the cGAS–STING pathway, which was evident with the upregulation of p-STING and p-IRF3. This also subsequently facilitated the formation of the AIM2/ASC inflammasome, which ultimately resulted in GSDMD-mediated canonical pyroptosis. Concurrently, **MC-13** and **MC-14** stimulated the KEAP1/NRF2/HO-1 pathway, which modifies endogenous iron metabolism and establishes a conducive environment for lipid peroxidation. This iron dysregulation serves as a vital molecular link between GSDME-mediated non-canonical pyroptosis and GPX4 depletion, thereby synergistically enhancing ferroptosis.

A cobalt(III)–cyclam prodrug (**MC-15**, Fig. 7) was developed with the STING agonist **MSA-2** tethered as a releasable payload to facilitate selective accumulation in cancer tissue and potent activation of the STING pathway.[155] **MC-15** exhibited stability under physiological conditions, whereas in the TME, it became locally activated, hence enhancing therapeutic selectivity and reducing off-target effects. The complex exhibited significant cytotoxicity against breast cancer cells, markedly inducing DNA fragmentation and activating the cGAS–STING pathway, as demonstrated by increased levels of STING, IRF3, and TBK1, along with their phosphorylated forms. To enhance the pharmacokinetic and therapeutic profile of **MC-15**, the complex was encapsulated in polymeric NPs. Upon administration in murine models, the NPs preferentially localised in cancer tissues, eliciting a vigorous anti-tumour immune response and considerably inhibiting tumour growth. In the combination therapy, the intravenous administration of **MC-15** NPs (3 mg CO_2 kg^{-1}) alongside the α-PD-1 (10 mg kg^{-1}) antibody resulted in negligible systemic toxicity and achieved nearly full tumour eradication.

Gold (Au) complexes demonstrated superior anticancer efficacy by inhibiting thioredoxin reductase (TrxR); however, their clinical advancement has been impeded by stability issues and adverse side effects.[156] Recent research efforts aim to tackle these issues by combining robust electron-donating ligands, such as N-heterocyclic carbenes (NHCs) and alkynyl groups, to stabilize the gold metal core. Moreover, anchoring targeting scaffolds enhances selectivity by guiding complexes to specific cells or compartments, thereby minimizing off-target effects.[157,158] Recently, a series of mitochondrial-targeting Au1-NHC complexes have been synthesized by combining the liver-targeting scaffold glycyrrhetinic acid (GA) with the mitochondria-directed TPP+ moiety.[159] Among them, complex **MC-16** demonstrated robust generation of ROS, which played a central role in triggering ICD (Fig. 8). Cellular studies reveal that **MC-16** is partially localized within the mitochondria and the ER and significantly alters the mitochondrial morphology and generates ROS, which not only induces cellular stress but also promotes the release of mtDNA into the cytoplasm. This cytoplasmic DNA acted as a potent activator of the cGAS–STING pathway, leading to the production of p-STING and p-NF-Kβ. The combined effect of ROS-induced ICD and cGAS–STING activation orchestrated a strong anticancer immune response, as evidenced by enhanced immune cell activation and cytotoxicity in both *in vitro* and *in vivo* experiments. Notably, intraperitoneal administration of **MC-16** (5 mg kg^{-1}) significantly suppressed tumour growth in a patient-derived xenograft model of hepatocellular carcinoma, highlighting its therapeutic potential as a dual-function agent that directly kills cancer cells and mobilizes anti-tumour immunity.

2.4 Nanomaterials incorporating the metal-based compounds to activate the cGAS–STING pathway

Nanotechnology offers significant benefits in augmenting drug solubility, boosting bioavailability, and minimizing systemic toxicity, rendering it a particularly appealing platform for cancer immunotherapy.[160–162] Nanomaterials, especially those that encapsulate or tether drugs, facilitate the targeted and sustained delivery of these agents to tumours, thereby augmenting innate and adaptive immune responses, enhancing APCs, and mitigating the immunosuppressive TME, ultimately improving the efficacy and safety of immune-based therapies.[163–166] In this section, we discussed the development (within the past two years) of nanomaterials that involve encapsulation or tethering of metal-based compounds to activate the cGAS–STING pathway and trigger the anti-tumour immune response.

A GSH-responsive nanoparticle, **NP2** (Fig. 9A), has recently been developed to co-deliver a platinum(IV) prodrug (Pt^{IV}-C12)

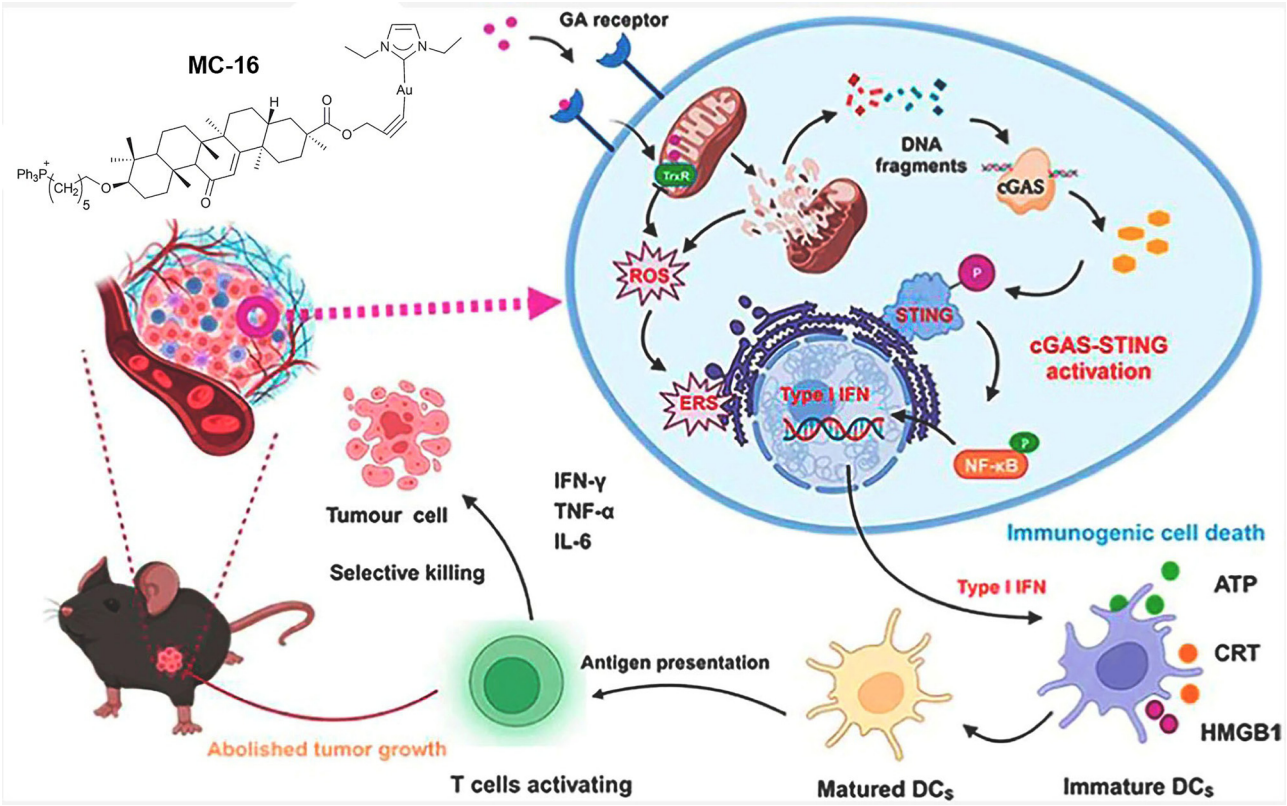

Fig. 8 Chemical structure of **MC-16** and a schematic representation of its capacity to activate STING pathways and elicit an immunological response. Adapted and modified with permission from ref. 159. Copyright 2024 American Chemical Society.

and a WEE1 kinase inhibitor (MK1775).[167] In the reductive TME, **NP2** releases its payload, resulting in the reduction of the encapsulated Pt^{IV} prodrug to active cDDP, which induces DNA damage and activates the cGAS–STING pathway, while MK1775 simultaneously inhibits DNA repair, yielding a synergistic effect that amplifies pathway activation. In comparison with free cDDP, **NP2** exhibited superior *in vitro* anti-tumour activity and, as demonstrated by RNA-seq, induced DNA damage, interfered with cell-cycle-related repair mechanisms, and activated the cGAS–STING pathway. Upon administration in a murine bladder cancer, **NP2** preferentially accumulated at tumour sites, suppressed tumour growth, and robustly activated STING signaling, which drove cytokine secretion, DC maturation, $CD8^+$ T-cell and NK-cell infiltration, M1-like polarization of macrophages, and reduced MDSC recruitment, effectively converting ''cold'' tumour into ''hot'' one. Additionally, **NP2** upregulated PD-L1 expression and, in combination with αPD-L1 therapy, significantly augmented splenic central memory T cells, strengthened immune memory, and suppressed metastasis and recurrence.

Recently, a polymer featuring a trisulfide bond (Poly3S) was engineered as a nanoparticle platform to encapsulate and deliver a Pt^{IV} prodrug, aiming to overcome cDDP resistance and reduce systemic toxicity.[168] Poly3S was synthesised using the condensation polymerisation of bis(2-hydroxyethyl) trisulfide and subsequently coassembled with a lipophilic Pt^{IV} prodrug to generate NPs (**NP(3S)s**, Fig. 9B). In 4T1 tumour cells, **NP(3S)s** administration resulted in increased Pt-DNA adducts compared to both cDDP and the Pt^{IV} prodrug, demonstrating a 9.1-fold increase over cDDP and a 2.1-fold rise over the Pt^{IV} prodrug. Flow cytometry and confocal imaging showed a significant increase in p–IRF3–positive cells, indicating strong activation of the STING signalling pathway. A transcriptomic study revealed that **NP(3S)s** treatment resulted in accumulation of oxidative stress and T-cell immunity, indicating a dual mechanism of intracellular GSH depletion and STING pathway activation. In 4T1 tumour-bearing mice, intravenous delivery of **NP(3S)s** led to selective tumour accumulation, reduced cisplatin-induced hepatotoxicity without affecting key organs, and achieved a 66.5% higher inhibition of subcutaneous breast tumour growth compared to cDDP. Immunohistochemistry, flow cytometry, and postsurgical rechallenge tests further validated an enhanced anti-tumour immune response and decreased tumour recurrence in **NP(3S)**-treated groups, underscoring the potential of Poly3S as a dual-function nanocarrier for Pt^{IV} based chemotherapy.

A synthetic high-density lipoprotein (sHDL) nanodisc was engineered for dual-modal imaging-guided distribution of a Pt^{IV} prodrug (Fig. 9C and D).[169] Administration of **sHDL@Pt** nanodiscs (hydrodynamic diameter = 10 nm) resulted in a 2.2-fold increase in dsDNA release compared to cDDP, exhibited improved TGI, and more effectively activated the cGAS–STING

pathway, as evidenced by significantly elevated phosphorylation levels of STING, IRF3, and TBK1 in 4T1 cells. Transcriptomic investigations also revealed that **sHDL@Pt** influenced the cGAS–STING pathway by causing DNA damage, modifying protein phosphorylation, and modulating the expression of pathway-related genes, consequently augmenting

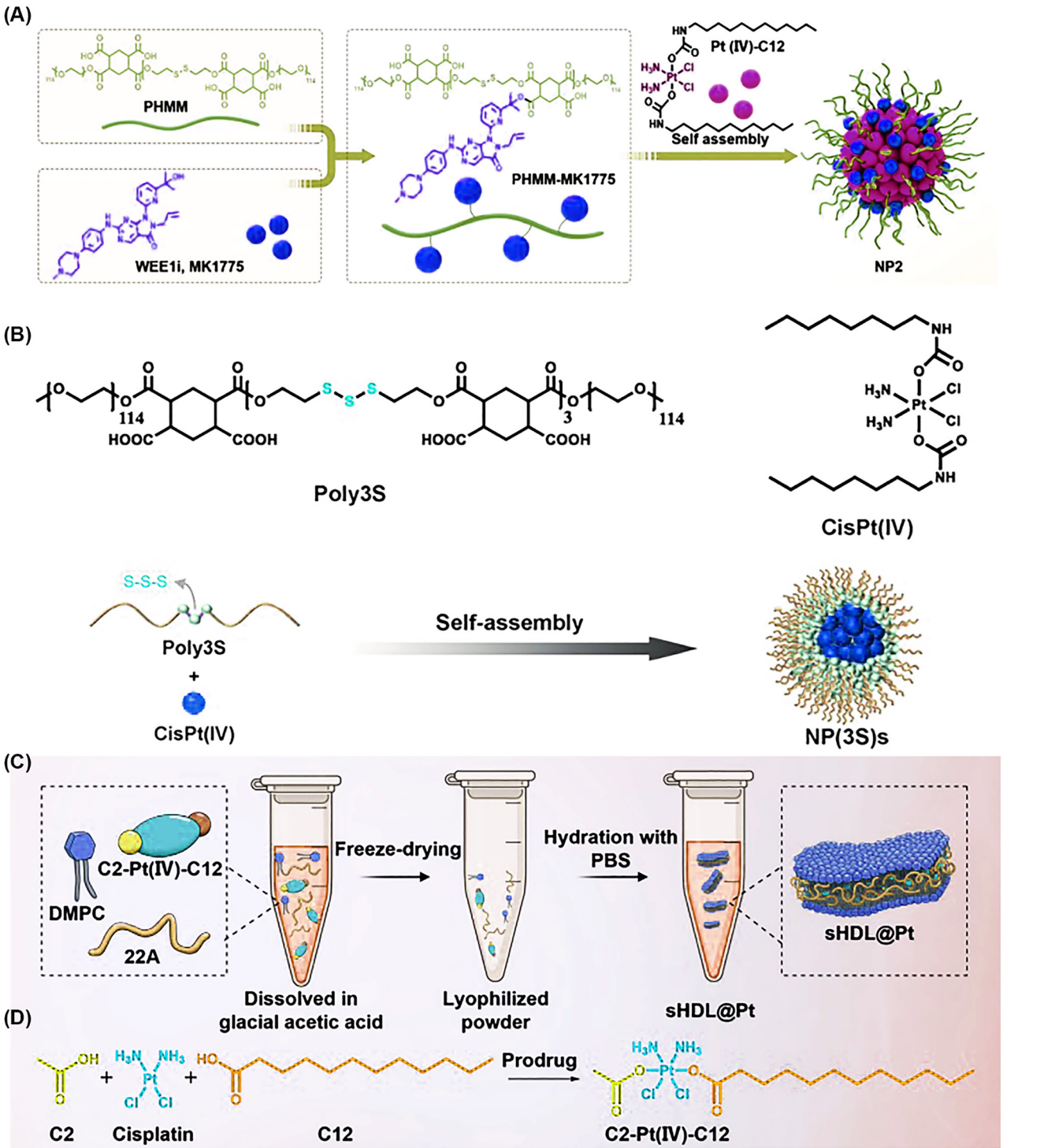

Fig. 9 Schematic depiction of the synthesis of the PHHM-MK1775 polymer–drug conjugate, accompanied by the incorporation of the Pt(IV)-C12 prodrug into the polymer matrix to produce **NP2** nanoparticles (A). Synthetic overview of redox-responsive polymers containing trisulfide bonds (Poly3S) used as carriers to encapsulate the Pt(IV) prodrug of cisplatin (CisPt(IV)), to form **(NP(3S)s)** nanoparticles (B). Illustrative overview of synthetic high-density lipoprotein-mimicking nanodiscs containing Pt(IV) prodrug (C2-Pt(IV)-C12) to activate the cGAS-STING pathway (C). The structural formula of the Pt(IV) prodrug (C2-Pt(IV)-C12) used in sHDL and its reduction process to Pt(II) *in vivo* (D). Adapted and modified with permission from ref. 167 (Copyright 2023 Wiley-VCH), **168** (Copyright 2025 American Chemical Society), and **169** (Copyright 2025 Wiley-VCH).

immune-stimulatory factors and transforming the immunosuppressive TME. In 4T1 mouse tumour models, **sHDL@Pt** (1.0 (kg BM)$^{-1}$) attained a TGI of 76%, in contrast to 57% for cDDP, and led to the total survival of treated animals, while the PBS- and cDDP-treated groups perished after 36 days. Combination therapy utilising **sHDL@Pt** and an anti-PD-1 antibody resulted in nearly complete tumour regression, attaining a TGI of 88%, signifying a synergistic impact that enhanced both cytotoxic and immune-mediated anti-tumour responses. The authors conclude that **sHDL@Pt** discs can function as a next-generation Pt^{IV} platform that integrates chemotherapy with immune checkpoint blockade, providing a flexible approach for precision immuno-oncology.

A pH- and redox-responsive nanomedicine, **DHP/MnO_2NPs**, was engineered to enhance the intratumoural accumulation and retention of Mn^{2+} ions, thereby promoting spatiotemporal synergy and significantly amplifying STING pathway activation and improving chemoimmunotherapy for lung cancer (Fig. 10A).[170] The nanomedicine was prepared using a novel platinum^{IV}-backboned polymer prodrug P(DHP-PEG). P(DHP-PEG), rich in carboxyl groups, efficiently and stably chelating Mn^{2+}, thus facilitating the formation of **DHP/MnO_2NPs**. Mechanistic studies revealed that **DHP/MnO_2NPs** released cDDP and Mn^{2+} ions in the TME, with cDDP causing DNA damage in tumour cells and then leaking into the cytoplasm, where it collaborated with Mn^{2+} to activate the STING pathway and downstream IRF3 and NF-κB signalling cascades. This activation resulted in significantly increased expression of IFN-β and several proinflammatory cytokines, triggering robust anticancer immune responses. In addition, **DHP/MnO_2NPs** efficiently reversed the immunosuppressive TME by triggering phenotypic remodelling of tumour-associated macrophages, leading to a significant increase in the infiltration of F4/80$^+$/CD86$^+$ pro-inflammatory macrophages. **DHP/MnO_2NPs** exhibited improved anticancer activity in both subcutaneous and metastatic orthotopic lung cancer murine models. Interestingly, pharmacological inhibition of STING signalling significantly diminished the anticancer effects and immunostimulatory activity of **DHP/MnO_2NPs**, thereby affirming the pivotal role of STING activation in facilitating the therapeutic benefits of the nanomedicine.

A rationally designed lipophilic Pt^{IV} prodrug (Cis-C8) and a structurally stable and cytotoxic manganese complex (**TPA-Mn**) were developed and co-formulated with DSPE-PEG2000 and a ROS-sensitive polymer (PCPP) to generate ROS-responsive self-assembled NPs (**NPPt**, **NPMn**, Fig. 10B).[171] MTT assay demonstrated that **NPMn** had a significantly lower IC_{50} value than cDDP across several cancer cell lines, highlighting its substantial anticancer efficacy, while **NPPt** revealed an even more pronounced inhibitory effect on tumour cell proliferation compared to **NPMn**. **TPA-Mn** activated cGAS independently of manganese ions and elicited significant anti-tumour effects, evidenced by a 1.6-fold increase in p-STING levels, which subsequently augmented the secretion of pro-inflammatory cytokines (TNF-α, IL-6, and IL-2), stimulated DC maturation, enhanced CTL infiltration, and reduced the proportion of immunosuppressive regulatory T cells. The intracellular conversion of Cis-C8 into the highly toxic parent compound, cDDP, induces DNA damage and facilitates the activation of the cGAS–STING pathway. Interestingly, the combined formulation (NPPt + NPMn) enhanced the reservoir of cGAS-sensitive dsDNA while damaging tumour cell DNA, resulting in the release of both the Cis-C8 prodrug and **TPA-Mn** to activate the cGAS–STING pathway and elicit a vigorous immune response. In conjunction with α-PD-1 therapy, **NPPt** + **NPMn** facilitated DC maturation, augmented CD8$^+$ T cell infiltration, diminished Tregs populations, and significantly amplified immune activation, thus inhibiting immune evasion and restructuring the tumour immune microenvironment in a model of advanced ovarian cancer peritoneal metastasis.

The use of three-dimensional (3D)-printed bone scaffolds for localised chemotherapeutic drug delivery has been increasingly popular in recent years, garnering significant attention as a component of a more comprehensive and integrated treatment approach for osteosarcoma (OS).[172–174] By keeping in view, Chen *et al.* developed a biodegradable 3D-printed bone scaffold platform intended to incorporate localised photothermal-chemotherapy, immune-synergistic therapy, and bone healing for OS treatment (Fig. 10C and D).[175] The scaffold was developed by initially synthesising a Pt^{IV} prodrug, which was covalently attached to polydopamine (PDA) using an amidation reaction to produce a composite nanomaterial (**PDA@Pt**). The nanomaterial was subsequently integrated into a poly(L-lactic acid)/bioactive glass matrix to produce a multifunctional composite utilising selective laser sintering technology. Structural investigation revealed that **PDA@Pt NPs** displayed a nearly spherical morphology with slightly rough edges and an average particle size of around 226.5 nm. Mechanical testing and *in vitro* assessments revealed that **PDA@Pt NPs** exhibited suitable compressive strength, elevated hydrophilicity, and significant mineralisation capability, while effectively inhibiting OS cell proliferation and viability upon light treatment (808 nm, 1.0 W cm^{-2}). Further mechanistic studies demonstrated that **PDA@Pt NPs** activate the cGAS–STING signalling pathway *via* DNA damage induction, which subsequently facilitates DC maturation and increased infiltration of cytotoxic CD8$^+$ T cells into tumour tissues, highlighting its potential for immune-synergistic therapy. In addition, the material demonstrated exceptional biocompatibility, osteoinductivity, and the ability to enhance osteogenic development of rat bone marrow mesenchymal stem cells. Long-term implantation studies demonstrated that the **PDA@Pt** scaffold biodegraded progressively over 12 weeks with minimal systemic toxicity. It markedly enhanced new bone formation at the defect site, underscoring its potential as a multifunctional therapeutic platform for concurrent cancer treatment and bone regeneration.

A nanophotosensitizer, **Ru-DNA@Lipo**, was developed by encapsulating plasmid DNA intercalated with the Ru^{II} complex (**RuDPPN**) within liposomes to induce photocleavage of the DNA that activates the cGAS–STING pathway (Fig. 11A).[176] Ru-DNA@Lipo demonstrated improved cellular uptake, likely due to the incorporation of DNA, which reduces the overall positive

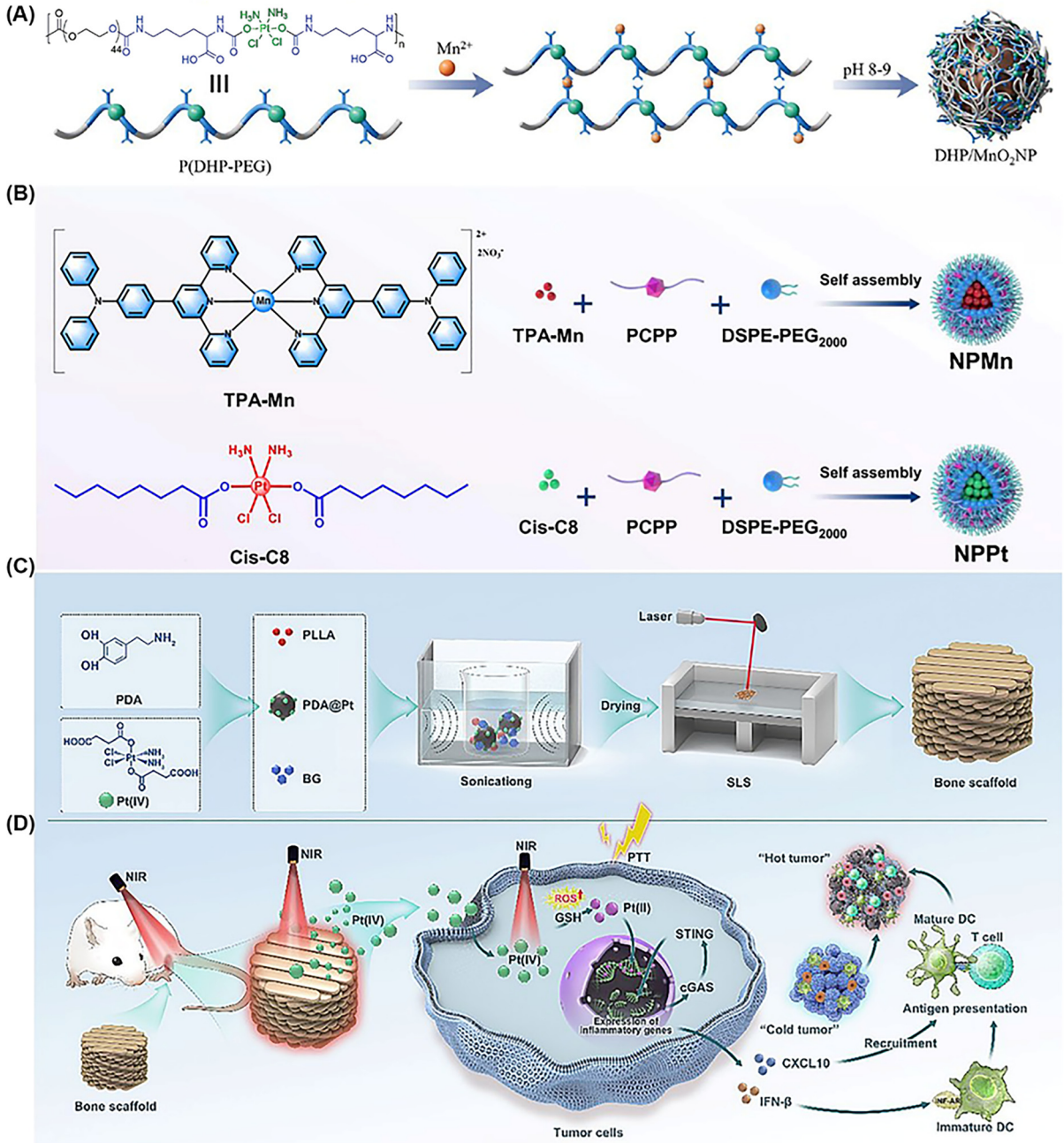

Fig. 10 Schematic representation of the fabrication of platinum(IV)-backboned polymer prodrug P(DHP-PEG)-coated MnO_2 nanoparticles (**DHP/MnO_2NP**) (A). Chemical structures of TPA-Mn and Cis-C8, along with their encapsulation in DSPE-PEG2000 and a ROS-sensitive polymer (PCPP), to produce **NPMn** and **NPPt** nanoparticles (B). Illustrative overview of 3D-printed bone scaffolds (**PDA@Pt NPs**) developed for OS treatment (C). Mechanistic insights into the STING activation by **PDA@Pt NPs** for OS targeted tumour immunotherapy (D). Adapted and modified with permission from ref. 170 and 171 (Copyright 2025 American Chemical Society) and **175** (Copyright 2025 Springer Nature).

charge and aids in membrane permeability. Following light exposure (450 nm, 7.5 mW cm^{-2}, 150 s), **Ru-DNA@Lipo** augmented the expression of cGAS, p-STING, and p-IRF3 proteins, which results in a 9.3-fold increase in extracellular IFN-β levels. Moreover, **Ru-DNA@Lipo** treatment resulted in a 220-fold elevation in extracellular ATP levels and prompted the translocation of CRT and HMGB1 proteins, thereby validating its capacity to induce ICD. The authors conclude that the combined delivery of DNA and DNA photocleavage agents to tumour cells is a viable approach for effective photodynamic immunotherapy.

Recently, an osmium–cyanine complex (**OsNIR**) had been developed with aggregation-dependent photodynamic–photothermal switching and was strategically encapsulated in ferritin to produce tumour-targeting **OsNIR@HFn NPs** (Fig. 11B).[177] TEM analysis revealed that the **OsNIR@HFn NPs** possessed a

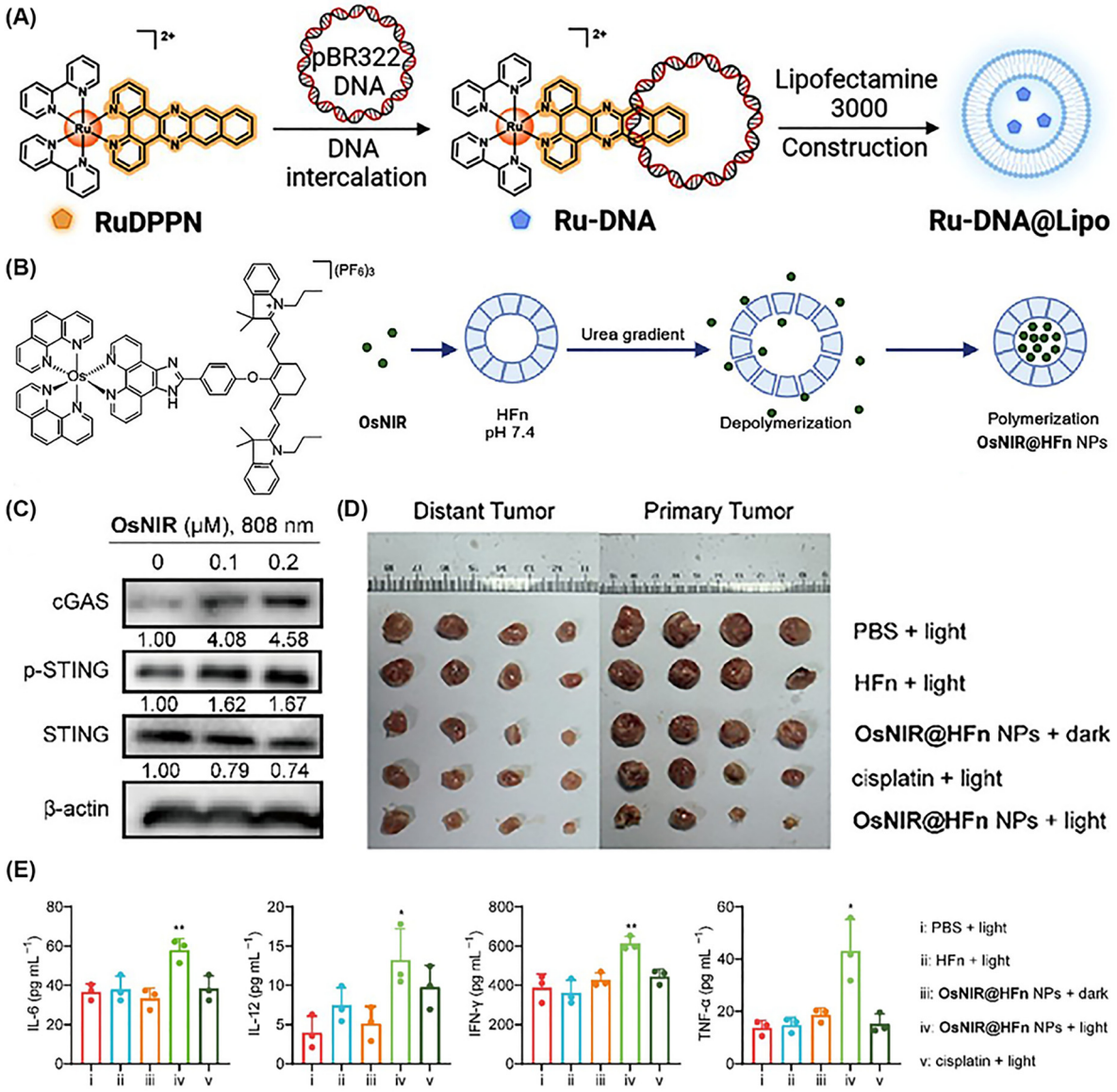

Fig. 11 Chemical structure of **RuDPPN** and illustrative overview of encapsulating plasmid DNA intercalated with the RuDPPN within liposomes (**Ru-DNA@Lipo**) (A). Chemical structure of **OsNIR** and its encapsulation in ferritin to produce tumour-targeting **OsNIR@HFn NPs** (B). Western blot images showing the effect of **OsNIR@HFn NPs** on the STING associated proteins (C). Photographs of primary and distant tumours after treatment with various formulations (D). The quantified concentration of IL-6, IL-12, IFN-γ, and TNF-α in mouse serum after treatment with various formulations (E). Adapted and modified with permission from ref. 176 and 177 (Copyright 2025 Wiley-VCH).

uniform and well-defined nanospherical morphology with an average diameter of approximately 10 nm. Cellular studies revealed that in the absence of light, OsNIR displayed cytotoxicities across various cancer cell lines in the range of 6.73–9.21 μM. Upon irradiation (808 nm), the IC_{50} values of OsNIR decreased dramatically to 0.04–0.13 μM, with calculated photocytotoxicity indices ranging from 67.77 to 168.25. In contrast, **OsNIR@HFn** NPs were considered essentially nontoxic under dark conditions, exhibiting IC_{50} values above 200 μg mL^{-1}, which indicated markedly improved biocompatibility relative to free OsNIR. When exposed to NIR light, the phototoxicities of **OsNIR@HFn NPs** fell within 3.12–6.12 μg mL^{-1}, demonstrating potent light-triggered therapeutic activity. Moreover, upon NIR treatment, the released OsNIR moieties induced extensive mtDNA damage, thereby triggering the cyclic cGAS–STING signaling pathway and leading to pronounced increases in the expression levels of cGAS and pSTING (Fig. 11C). *In vivo* experiments further confirmed that **OsNIR@HFn NPs** were highly effective for real-time bioimaging and metabolic tracking while also demonstrating significant TGI (Fig. 11D). Cytokine profiling of murine serum revealed robust upregulation of key proinflammatory mediators following **OsNIR@HFn** NP-mediated phototherapy, with notable elevations in IL-12, IL-6, TNF-α, and IFN-γ compared with baseline levels (Fig. 11E). Collectively, these findings indicated that after treatment of 4T1 tumour-bearing mice with **OsNIR@HFn NPs**, the

infiltration of immune cells within the TME was markedly enhanced, effectively converting the immunologically "cold" tumour phenotype into a more responsive "hot" tumour state.

3. Conclusions, challenges and future directions

Since the discovery of STING and cGAS, the scientific understanding of the cGAS–STING DNA sensing pathway has been substantially improved in bridging innate and adaptive immunity, rendering it a promising target for orchestrating anti-tumour immune responses. Given its central immunomodulatory function, cGAS–STING agonists serve as promising therapeutic agents. They can enhance both innate and adaptive anti-tumour immunity when used alone or in combination with ICIs or chemotherapeutics to augment treatment efficacy across diverse tumours. This review emphasises and examines various STING agonists under investigation for therapeutic development, including well-known natural and synthetic CDNs, as well as recently developed (within the past two years) small organic compounds, metal-based complexes, and nanomaterials tethering or encapsulating metal-based drugs. These compounds exemplify several structural classes and molecular approaches designed to modulate STING signalling for cancer immunotherapy. Although present research on STING-based immunotherapy is limited, the concept has tremendous potential for future development. For instance, CDNs activate the STING pathway, resulting in enhanced production of IFN-I and proinflammatory cytokines, thereby improving DC maturation, APC function, and $CD8^+$ T lymphocyte priming. While animal models demonstrate significant efficacy, clinical results involving CDN-based STING agonists have been disappointing. For example, **ADU-S100** (MIW815) exhibited a response rate of merely 2.1%, comparable to that of untreated control groups.[50] Another CDN-based STING agonist, **MK-1454**, exhibited negligible anticancer efficacy. When combined with the anti PD-1 monoclonal antibody pembrolizumab, **MK-1454** exhibited an overall response rate of 24%. However, patients experienced severe TRAEs, and some of them had to discontinue therapy prematurely due to toxicity. These clinical challenges can be further explained by translational factors, including hSTING polymorphism-dependent variability and the pharmacokinetic behaviour of CDNs. hSTING harbours several common functional variants (*e.g.*, WT, R232H, HAQ, AQ, and R293Q) that exhibit markedly different responsiveness to CDNs, with reported differences in activation potency of up to an order of magnitude, contributing to substantial inter-individual variability in immune responses.[178,179] Certain mutations, such as R232H and HAQ, directly reshape the ligand-binding pocket of STING, preventing conventional CDNs from effective binding or proper conformational activation. These variants also disrupt key downstream processes including STING dimerization, Golgi translocation, TBK1 recruitment, and IRF3 phosphorylation, leading to pronounced differences in cytokine production (*e.g.*, IFN-β, IL-6, and TNF-α).[180,181] Moreover, following intratumoral administration, CDNs are rapidly cleared *via* lymphatic drainage and display limited intratumoral diffusion due to their small size and high hydrophilicity, potentially leading to incomplete tumor coverage, insufficient immune activation at invasive margins, and marginal tumor recurrence.[49] Collectively, these genetic and pharmacokinetic limitations underscore the challenges in achieving consistent and effective STING activation with conventional CDNs.

In addition to CDNs, several organic scaffolds have been developed as STING agonists. Among these, **DMXAA**, **SR-717Z**, and **MSA-2** are the pioneers, with the latter being the first orally formulated STING agonist. These compounds cross the cellular membrane and enter the cytosol by passive diffusion, thereby avoiding the need for active transport or endosomal uptake. They stimulate STING, which leads to overproduction of IFN-I and, as a result, an anti-tumour immune response. A diverse array of new structural analogues of **DMXAA** and **SR-717** have recently been identified, demonstrating substantial improvements in anti-tumour efficacy (Fig. 4). These agents successfully activate the cGAS–STING signalling pathway, leading to partial or complete tumour eradication in murine models, and their therapeutic efficacy surpasses that of their parent compounds, underscoring their potential as promising candidates for advancing STING-targeted cancer immunotherapy. Moreover, PSs have been engineered, which, upon activation with appropriate light, induce elevated levels of pSTING and activate many STING-associated proteins and trigger ICD through the production of DAMPs. Determining the most promising compound among them is challenging, as they are not clinically approved, and the field is advancing rapidly with significant potential to enhance cancer immunotherapy.

Metal-based compounds exhibit significant therapeutic potential, especially in combination therapies that incorporate metallodrugs with ICIs or metabolic modifiers.[182] As a result, there has been a growing scientific focus on the rational design and synthesis of metallodrugs capable of independently activating the cGAS–STING pathway or, when conjugated with STING agonists, enhancing anticancer immune responses. In this context, several metal-based compounds, including Pt^{II}, Cu, Ir, Ru, and Rh, have been developed that inherently interact with and damage DNA through covalent binding, intercalation, or ROS generation, which can lead to cytosolic leakage of DNA fragments and subsequent activation of the cGAS–STING pathways (Fig. 7). Additionally, rationally designed Pt^{IV} and Co complexes have been developed and investigated to achieve synergistic immunostimulation by conjugating a STING agonist (**MSA-2**), thereby integrating DNA-targeting cytotoxicity with direct STING activation. These dual-acting metal complexes constitute a promising approach for cancer immunotherapy, utilising both DNA-mediated immunogenicity and STING-induced immune activation to enhance anti-tumour immunity.

The encapsulation or tethering of metal-based compounds into or within the polymer-based delivery vehicles has emerged as an attractive strategy to activate the STING pathway, as it improves the stability, bioavailability, and targeted delivery of

the metal compounds while minimizing systemic toxicity and enhancing cellular uptake. Metal complexes play a pivotal role in these polymer-based nanosystems, as many encapsulate Pt^{IV} complexes which, upon release and subsequent intracellular reduction to their active parental Pt^{II} forms, induce DNA damage and activate the STING pathway. In addition to Pt complexes, Ru and Os metal-based PSs have also been encapsulated into drug delivery vehicles. Upon release and photoactivation under specific light irradiation, these PSs generate ROS that not only cause ICD but also promote cytosolic DNA leakage and oxidative stress, thereby activating the cGAS–STING signaling cascade and enhancing anti-tumour immune responses. Co-administration with ICIs, such as anti PD-1 monoclonal antibodies, enables some of these nanosystems to elicit a synergistic therapeutic effect by converting immunologically 'cold' tumours into 'hot' tumours.

Despite significant scientific advancements and the increasing therapeutic potential of cGAS–STING agonists, no drug from this class has yet received clinical approval. The trajectory towards successful drug development is challenging, mainly due to concerns over the chemical and biological compatibility of these compounds as well as the inter-species TME heterogeneity. For instance, due to the structural differences between hSTING and mSTING, outcomes from animal models sometimes fail to adequately represent human conditions. An explicit example is the compound **DMXAA**, which robustly activates STING in murine models but exerts no influence on hSTING. In addition to these distinctions, numerous early STING agonists, particularly free CDNs, exhibit poor pharmacokinetic profiles and lack selectivity, leading to indiscriminate STING activation in both tumour and normal tissues, potentially inducing excessive inflammatory responses and causing systemic toxicity. The pro-inflammatory effects can be intensified when used alongside ICIs, increasing the likelihood of a cytokine storm. Moreover, hyperactivation of the STING pathway may lead to temporary over-stimulation of T cells, potentially disrupting immunological tolerance and triggering autoimmune reactions.[183,184] In addition, from a translational perspective, nanomedicine faces numerous significant challenges. A major challenge is scaling up production from laboratory to industrial levels while maintaining the physicochemical properties and medicinal efficacy of nanoparticles. Moreover, maintaining the long-term physical and chemical stability of nanoformulations during storage and transportation is a continual challenge, as nanoparticles may aggregate, degrade, or undergo surface alterations over time, thereby jeopardising their safety and efficacy. Addressing all these challenges, particularly through strategies to reduce inflammation and prolong the therapeutic window, is crucial for realising the full clinical potential of this intriguing class of compounds.

As research in this fast advancing field progresses, a more profound and comprehensive understanding of the immunopharmacological processes regulating the cGAS–STING pathway is expected. Emerging research methodologies for STING agonist discovery increasingly combine SAR-guided optimization with advanced computer-aided drug design (CADD) strategies. Modern CADD frameworks integrate quantum-mechanical calculations, molecular dynamics simulations, and binding free-energy analyses to capture both ligand-specific interactions and the dynamic nature of STING activation, including ligand-induced conformational rearrangements and cooperative binding effects.[185] Leveraging cocrystal structures of well-characterized STING agonists as structural templates, these computational approaches enable *in silico* prediction of binding modes, key intermolecular interactions, and relative binding affinities prior to synthesis, thereby prioritizing promising candidates for experimental validation.[80] Guided by these computational frameworks, potential structural modifications may be explored to improve drug-like properties, such as enhancing cellular permeability and oral bioavailability by reducing polar functionalities (–OH, –COOH, and $–NH_2$), introducing lipophilic substituents ($–CH_3$, $–OCH_3$, and halogens), or transiently masking charged groups through ester or amide prodrug strategies.

Additionally, fine-tuning steric bulk, hydrogen-bond donor/acceptor patterns, and electronic properties of aromatic or heterocyclic motifs can be used to balance STING activation potency while mitigating excessive systemic cytokine release and associated toxicities. Such control over the pharmacological and immunostimulatory profile of STING agonists is particularly important for their safe and effective deployment in combination regimens, where uncontrolled innate immune activation could exacerbate adverse effects. In this context, the strategic integration of STING agonists with ICIs, chemotherapeutic drugs, and DNA-damaging agents achieves synergistic or multiplexed stimulation of anti-tumour immunity. Moreover, elucidating the interplay between STING signalling and other cell death pathways such as ferroptosis, pyroptosis, and necroptosis will illuminate new regulatory networks that influence immune-tumour interactions. Furthermore, the development of metal-based PS is crucial for selectively activating the STING pathway, while also mitigating the cytokine storm that can arise from excessive STING activation. Advanced analytical technologies, such as single-cell transcriptomics and spatial proteomics, will be crucial for elucidating the cellular and spatial heterogeneity of the TME, thereby facilitating a more accurate understanding of how STING activation influences immune cell recruitment and tumour immunogenicity. The advancement of intelligent delivery platforms can facilitate controlled, site-specific release of STING agonists, enhancing therapeutic precision and minimising systemic toxicity. These innovative strategies will enhance the efficiency, specificity, and safety of STING-based immunotherapies while bridging the translational gap between strong preclinical results and inconsistent clinical outcomes, facilitating the development of the next generation of immunemodulatory cancer treatments.

Conflicts of interest

There are no conflicts to declare.

Data availability

There are no original data in this manuscript to make available.

Acknowledgements

This work was supported by the Fundamental Research Funds for the Central Universities (3072024CFJ1003) and the Natural Science Foundation of China (grant U22A20347). MH thanks the Health Research Council of New Zealand for a Sir Charles Hercus Health Research Fellowship.

References

1 R. Wang, C. Lan, K. Benlagha, N. O. S. Camara, H. Miller, M. Kubo, S. Heegaard, P. Lee, L. Yang, H. Forsman, X. Li, Z. Zhai and C. Liu, *MedComm*, 2024, **5**, e714.
2 T. Pradeu, B. P. H. J. Thomma, S. E. Girardin and B. Lemaitre, *Immunity*, 2024, **57**, 613–631.
3 T. Matsunaga and A. Rahman, *Immunol. Rev.*, 1998, **166**, 177–186.
4 T. Boehm, *Curr. Biol.*, 2012, **22**, R722–R732.
5 M. D. Cooper and M. N. Alder, *Cell*, 2006, **124**, 815–822.
6 T. Boehm, *Nat. Rev. Immunol.*, 2025, **25**, 141–152.
7 D. S. Michaud, E. A. Houseman, C. J. Marsit, H. H. Nelson, J. K. Wiencke and K. T. Kelsey, *Cancer Epidemiol. Biomarkers Prev.*, 2015, **24**, 1811–1819.
8 H. Garner and K. E. de Visser, *Nat. Rev. Immunol.*, 2020, **20**, 483–497.
9 M. Jiang, H. Fang and H. Tian, *Theranostics*, 2025, **15**, 155–188.
10 C. Galassi, T. A. Chan, I. Vitale and L. Galluzzi, *Cancer Cell*, 2024, **42**, 1825–1863.
11 L. Galluzzi, *Nat. Rev. Immunol.*, 2025, **25**, 227–228.
12 M. Nafees, M. Hanif and P. Yang, *Chin. Chem. Lett.*, 2025, 111013.
13 R. J. Davis, C. Van Waes and C. T. Allen, *Oral Oncol.*, 2016, **58**, 59–70.
14 Y. Jin, Y. Huang, H. Ren, H. Huang, C. Lai, W. Wang, Z. Tong, H. Zhang, W. Wu, C. Liu, X. Bao, W. Fang, H. Li, P. Zhao and X. Dai, *Biomaterials*, 2024, **305**, 122463.
15 R. Liu, J. Li, L. Liu, W. Wang and J. Jia, *Cancer Pathog. Ther.*, 2025, **3**, 183–196.
16 F. Wang, K. Fu, Y. Wang, C. Pan, X. Wang, Z. Liu, C. Yang, Y. Zheng, X. Li, Y. Lu, K. K. W. To, C. Xia, J. Zhang, Z. Shi, Z. Hu, M. Huang and L. Fu, *Acta Pharm. Sin. B*, 2024, **14**, 905–952.
17 D. Deng, M. Wang, Y. Su, H. Fang, Y. Chen and Z. Su, *J. Med. Chem.*, 2024, **67**, 6810–6821.
18 C. Verma, V. A. Pawar, S. Srivastava, A. Tyagi, G. Kaushik, S. K. Shukla and V. Kumar, *Vaccines*, 2023, **11**(12), 1783.
19 P. Liao, Y. Zhou, Y. Qiu, R. Hu, H. Li, H. Sun and Y. Li, *Cancer Metastasis Rev.*, 2025, **44**, 49.
20 B. Liu, X. Chen, Y. Zhu, H. Chen, J. Tan, Z. Yang, J. Li, P. Zheng, L. Feng, Q. Wang, S. Gai, L. Zhong, P. Yang, Z. Cheng and J. Lin, *Adv. Mater.*, 2025, **37**, 2500337.
21 C. Chen and P. Xu, *Trends Cell Biol.*, 2023, **33**, 630–648.
22 S. Wang, L. Qin, F. Liu and Z. Zhang, *Cell Commun. Signaling*, 2025, **23**, 171.
23 Z. Liu, D. Wang, J. Zhang, P. Xiang, Z. Zeng, W. Xiong and L. Shi, *Cancer Lett.*, 2023, **577**, 216409.
24 Y. Tang, W. Wang and C. Chen, *Commun. Biol.*, 2025, **8**, 541.
25 Y. Liu and P. Xu, *Cell Insight*, 2025, **4**, 100249.
26 Q. Yin, Y. Tian, V. Kabaleeswaran, X. Jiang, D. Tu, M. J. Eck, Z. J. Chen and H. Wu, *Mol. Cell*, 2012, **46**, 735–745.
27 L. Sun, J. Wu, F. Du, X. Chen and Z. J. Chen, *Science*, 2013, **339**, 786–791.
28 K.-P. Hopfner and V. Hornung, *Nat. Rev. Mol. Cell Biol.*, 2020, **21**, 501–521.
29 H. Ishikawa and G. N. Barber, *Nature*, 2008, **455**, 674–678.
30 J. He and L. Zhang, *Cytokine Growth Factor Rev.*, 2024, **78**, 25–36.
31 S. Skopelja-Gardner, J. An and K. B. Elkon, *Nat. Rev. Nephrol.*, 2022, **18**, 558–572.
32 C. Zhang, G. Shang, X. Gui, X. Zhang, X.-C. Bai and Z. J. Chen, *Nature*, 2019, **567**, 394–398.
33 T. Abe and N. Barber Glen, *J. Virol.*, 2014, **88**, 5328–5341.
34 Q. Wang, Y. Yu, J. Zhuang, R. Liu and C. Sun, *Mol. Cancer*, 2025, **24**, 178.
35 S. Yum, M. Li, Y. Fang and Z. J. Chen, *Proc. Natl. Acad. Sci. U. S. A.*, 2021, **118**(14), e2100225118.
36 C. Fu, H. Guo, M. Wang, C. Ni, X. Wu, X. Chen, J. Hou and L. Wang, *Int. Immunopharmacol.*, 2024, **143**, 113591.
37 A. Takaoka, S. Hayakawa, H. Yanai, D. Stoiber, H. Negishi, H. Kikuchi, S. Sasaki, K. Imai, T. Shibue, K. Honda and T. Taniguchi, *Nature*, 2003, **424**, 516–523.
38 M. Ghosh, S. Saha, J. Li, D. C. Montrose and L. A. Martinez, *Mol. Cell*, 2023, **83**, 266–280.e266.
39 K. R. B. Lanng, E. L. Lauridsen and M. R. Jakobsen, *Nat. Immunol.*, 2024, **25**, 1144–1157.
40 S. Gerondakis, T. S. Fulford, N. L. Messina and R. J. Grumont, *Nat. Immunol.*, 2014, **15**, 15–25.
41 S. E. Barnes, Y. Wang, L. Chen, L. L. Molinero, T. F. Gajewski, C. Evaristo and M. L. Alegre, *J. Immunother. Cancer*, 2015, **3**, 1.
42 H. Mao, X. Zhao and S.-C. Sun, *Cell. Mol. Immunol*, 2025, **22**, 811–839.
43 T. Liu, L. Zhang, D. Joo and S.-C. Sun, *Signal Transduction Targeted Ther.*, 2017, **2**, 17023.
44 H. Yu, L. Lin, Z. Zhang, H. Zhang and H. Hu, *Signal Transduction Targeted Ther.*, 2020, **5**, 209.
45 A. Amouzegar, M. Chelvanambi, J. N. Filderman, W. J. Storkus and J. J. Luke, *Cancers*, 2021, **13**, 2695.
46 M. Smith, D. Chin, S. Chan, S. Mahady, L. Campion, C. Morgan, S. Patel, G. Chu, A. Hughes, G. Bignan, P. Connolly, S. Emanuel, K. Packman and L. L. Luistro, *Cancer Res.*, 2020, **80**, 5567.
47 M. Su, J. Zheng, L. Gan, Y. Zhao, Y. Fu and Q. Chen, *Biochem. Pharmacol.*, 2022, **198**, 114934.
48 A. T. Whiteley, J. B. Eaglesham, C. C. de Oliveira Mann, B. R. Morehouse, B. Lowey, E. A. Nieminen, O. Danilchanka,

D. S. King, A. S. Y. Lee, J. J. Mekalanos and P. J. Kranzusch, *Nature*, 2019, **567**, 194–199.
49 J. Wang, F. Meng and Y. Yeo, *Curr. Opin. Biotechnol.*, 2024, **87**, 103105.
50 F. Meric-Bernstam, S. K. Sandhu, O. Hamid, A. Spreafico, S. Kasper, R. Dummer, T. Shimizu, N. Steeghs, N. Lewis, C. C. Talluto, S. Dolan, A. Bean, R. Brown, D. Trujillo, N. Nair and J. J. Luke, *J. Clin. Oncol.*, 2019, **37**, 2507.
51 C. Ding, Z. Song, A. Shen, T. Chen and A. Zhang, *Acta Pharm. Sin. B*, 2020, **10**, 2272–2298.
52 K. J. Harrington, J. Brody, M. Ingham, J. Strauss, S. Cemerski, M. Wang, A. Tse, A. Khilnani, A. Marabelle and T. Golan, *Ann. Oncol.*, 2018, **29**, viii712.
53 H. Gogoi, S. Mansouri and L. Jin, *Vaccines*, 2020, **8**(3), 453.
54 C. Huang, T. Tong, L. Ren and H. Wang, *Chembiochem*, 2024, **25**, e202400255.
55 L. Motedayen Aval, J. E. Pease, R. Sharma and D. J. Pinato, *J. Clin. Med.*, 2020, **9**, 3323.
56 J. J. Luke, D. J. Pinato, D. Juric, P. LoRusso, P. J. Hosein, A. M. Desai, R. Haddad, M. de Miguel, A. Cervantes, W. S. Kim, A. Marabelle, Y. Zhang, Y. Rong, X. Yuan and S. Champiat, *J. Immunother. Cancer*, 2025, **13**, e010511.
57 C. Huang, N. Shao, Y. Huang, J. Chen, D. Wang, G. Hu, H. Zhang, L. Luo and Z. Xiao, *Mater. Today Bio*, 2023, **23**, 100839.
58 K. M. Garland, T. L. Sheehy and J. T. Wilson, *Chem. Rev.*, 2022, **122**, 5977–6039.
59 E. Carideo Cunniff, Y. Sato, D. Mai, V. A. Appleman, S. Iwasaki, V. Kolev, A. Matsuda, J. Shi, M. Mochizuki, M. Yoshikawa, J. Huang, L. Shen, S. Haridas, V. Shinde, C. Gemski, E. R. Roberts, O. Ghasemi, H. Bazzazi, S. Menon, T. Traore, P. Shi, T. D. Thelen, J. Conlon, A. O. Abu-Yousif, C. Arendt, M. H. Shaw and M. Okaniwa, *Cancer Res. Commun.*, 2022, **2**, 489–502.
60 A. J. Olszanski, J. J. Luke, P. M. LoRusso, G. S. Falchook, P. L. Bedard, R. E. Sanborn, S. P. Patel, D. Orr, J. P. Gibbs, C. Li, Y. C. Huang, R. Gregory, S. Perera, R. Xu, A. Joshi, M. Y. Lee, J. Raizer and X. Gao, *Ann. Oncol.*, 2023, **34**, S625–S626.
61 K. Rajasekaran, T. J. Ow, C.-A. O. Nathan, A. L. Tang, V. Mehta, B. A. Schiff, J. Pang, A. van Zante, A. Turner, M. Grenley, C. Burns, A. Merrell, E. Beirne, J. M. J. Derry, N. J. Schauer, J. P. Frazier, W. E. A. Jenkins, R. C. Gregory, N. Lineberry and R. A. Klinghoffer, *J. Clin. Oncol.*, 2023, **41**(16), 2579.
62 H. Vasiyani and B. Wadhwa, *Cell. Signalling*, 2025, **128**, 111647.
63 K. Liu, Y. Lan, X. Li, M. Li, L. Cui, H. Luo and L. Luo, *Biomed. Pharmacother.*, 2020, **132**, 110945.
64 X. Tian, F. Xu, Q. Zhu, Z. Feng, W. Dai, Y. Zhou, Q.-D. You and X. Xu, *Eur. J. Med. Chem.*, 2022, **244**, 114791.
65 D. Prantner, D. J. Perkins, W. Lai, M. S. Williams, S. Sharma, K. A. Fitzgerald and S. N. Vogel, *J. Biol. Chem.*, 2012, **287**, 39776–39788.
66 P. Gao, M. Ascano, T. Zillinger, W. Wang, P. Dai, A. A. Serganov, B. L. Gaffney, S. Shuman, R. A. Jones, L. Deng, G. Hartmann, W. Barchet, T. Tuschl and D. J. Patel, *Cell*, 2013, **154**, 748–762.
67 L. Corrales, L. H. Glickman, S. M. McWhirter, D. B. Kanne, K. E. Sivick, G. E. Katibah, S.-R. Woo, E. Lemmens, T. Banda, J. J. Leong, K. Metchette, T. W. Dubensky and T. F. Gajewski, *Cell Rep.*, 2015, **11**, 1018–1030.
68 S. Hou, X.-j Lan, W. Li, X.-l Yan, J.-j Chang, X.-h Yang, W. Sun, J.-h Xiao and S. Li, *Bioorg. Chem.*, 2020, **95**, 103556.
69 S. Hou, J. Chang, C. Xing, Z. Ye, W. Li, Y. Zhang, Z. Zheng, J. Xiao and S. Li, *J. Med. Chem.*, 2025, **68**, 9407–9430.
70 H. Y. Zhao, Z. Liu, J. Tao, S. Mao, M. Wang, M. He, B. Wen, W. Gao and D. Sun, *Cell Chem. Biol.*, 2025, **32**, 280–290.e214.
71 B.-S. Pan, S. A. Perera, J. A. Piesvaux, J. P. Presland, G. K. Schroeder, J. N. Cumming, B. W. Trotter, M. D. Altman, A. V. Buevich, B. Cash, S. Cemerski, W. Chang, Y. Chen, P. J. Dandliker, G. Feng, A. Haidle, T. Henderson, J. Jewell, I. Kariv, I. Knemeyer, J. Kopinja, B. M. Lacey, J. Laskey, C. A. Lesburg, R. Liang, B. J. Long, M. Lu, Y. Ma, E. C. Minnihan, G. O'Donnell, R. Otte, L. Price, L. Rakhilina, B. Sauvagnat, S. Sharma, S. Tyagarajan, H. Woo, D. F. Wyss, S. Xu, D. J. Bennett and G. H. Addona, *Science*, 2020, **369**, eaba6098.
72 J. Yang, Z. Luo, J. Ma, Y. Wang and N. Cheng, *J. Controlled Release*, 2024, **371**, 273–287.
73 H.-Y. Zhao, J. Tao, L. Zhang, Q. Li, M. He, B. Wen, Z. Liu, H. Myatt and D. Sun, *J. Med. Chem.*, 2025, **68**, 11365–11385.
74 M. Banerjee, S. Middya, R. Shrivastava, S. Basu, R. Ghosh, D. C. Pryde, D. B. Yadav and A. Surya, *PLoS One*, 2020, **15**, e0237743.
75 S. Basu, S. Middya, M. Banerjee, R. Ghosh, D. C. Pryde, D. B. Yadav, R. Shrivastava and A. Surya, *Eur. J. Med. Chem.*, 2022, **229**, 114087.
76 D. C. Pryde, S. Middya, M. Banerjee, R. Shrivastava, S. Basu, R. Ghosh, D. B. Yadav and A. Surya, *Eur. J. Med. Chem.*, 2021, **209**, 112869.
77 S. Basu, S. Middya, R. Shrivastava, D. C. Pryde, R. Ghosh, D. B. Yadav, M. Banerjee and A. Surya, *Eur. J. Med. Chem.*, 2025, **290**, 117577.
78 M. Zhao, W. Fan, Y. Wang, P. Qiang, Z. Zheng, H. Shan, M. Zhang, P. Liu, Y. Wang, G. Li, M. Li and L. Hong, *Eur. J. Med. Chem.*, 2024, **264**, 116018.
79 X. Wang, Z. Zhan, Z. Wang, Y. Zhang, K. Zhao, H. Li, X. Zhou, Y. Guo, F. Fan, J. Ding, M. Geng, X. Yu, W. Duan and Z. Xie, *MedComm*, 2025, **6**, e70001.
80 E. N. Chin, C. Yu, V. F. Vartabedian, Y. Jia, M. Kumar, A. M. Gamo, W. Vernier, S. H. Ali, M. Kissai, D. C. Lazar, N. Nguyen, L. E. Pereira, B. Benish, A. K. Woods, S. B. Joseph, A. Chu, K. A. Johnson, P. N. Sander, F. Martínez-Peña, E. N. Hampton, T. S. Young, D. W. Wolan, A. K. Chatterjee, P. G. Schultz, H. M. Petrassi, J. R. Teijaro and L. L. Lairson, *Science*, 2020, **369**, 993–999.
81 B. Shan, H. Hou, K. Zhang, R. Li, C. Shen, Z. Chen, P. Xu, R. Cui, Z. Su, C. Zhang, R. Yang, G. Zhou, Y. Liu, H. Guo, K. Chen, W. Fu, H. Jiang, S. Zhang and M. Zheng, *J. Med. Chem.*, 2023, **66**, 3327–3347.

82 H. Hou, J. Zhou, Q. Sui, C. Zhang, Z. Su, R. Cui, B. Shan, P. Xu, Z. Chen, B. Jiang, M. Li, K. Zhang, Y. Wang, N. Ma, D. Teng, M. Zheng and S. Zhang, *J. Med. Chem.*, 2025, **68**, 9864–9885.
83 M. Sun, K. Müllen and M. Yin, *Chem. Soc. Rev.*, 2016, **45**, 1513–1528.
84 Z. Yang and X. Chen, *Acc. Chem. Res.*, 2019, **52**, 1245–1254.
85 X. Lou, H. Wang, Y. Liu, Y. Huang, Z. Liu, W. Zhang and T. Wang, *Angew. Chem., Int. Ed.*, 2023, **62**, e202214586.
86 X. Zhao, R. Zheng, B. Zhang, Y. Zhao, W. Xue, Y. Fang, Y. Huang and M. Yin, *Angew. Chem., Int. Ed.*, 2024, **63**, e202318799.
87 D. Varshney, J. Spiegel, K. Zyner, D. Tannahill and S. Balasubramanian, *Nat. Rev. Mol. Cell Biol.*, 2020, **21**, 459–474.
88 D. Song, J. Luo, X. Duan, F. Jin and Y.-J. Lu, *Int. J. Biol. Macromol.*, 2025, **297**, 139896.
89 V. J. Sahayasheela, Z. Yu, T. Hidaka, G. N. Pandian and H. Sugiyama, *Trends Genet.*, 2023, **39**, 15–30.
90 G.-X. Tang, M.-L. Li, C. Zhou, Z.-S. Huang, S.-B. Chen, X.-C. Chen and J.-H. Tan, *Cell Chem. Biol.*, 2024, **31**, 1800–1814.e1807.
91 S. Marzano, G. Pinto, A. Di Porzio, J. Amato, A. Randazzo, A. Amoresano and B. Pagano, *Commun. Chem.*, 2025, **8**, 64.
92 X.-D. Wang, Y.-S. Liu, M.-D. Chen and M.-H. Hu, *Eur. J. Med. Chem.*, 2024, **269**, 116361.
93 M. Overchuk, R. A. Weersink, B. C. Wilson and G. Zheng, *ACS Nano*, 2023, **17**, 7979–8003.
94 Z. Hu, J. Li, L. Feng, Y. Zhu, R. Zhao, C. Yu, R. Xu, W. Wang, H. Ding and P. Yang, *Nano Lett.*, 2024, **24**, 16426–16435.
95 M. Li, J. Xiong, Y. Zhang, L. Yu, L. Yue, C. Yoon, Y. Kim, Y. Zhou, X. Chen, Y. Xu, X. Peng and J. S. Kim, *Chem. Soc. Rev.*, 2025, **54**, 7025–7057.
96 M. Jia, Y. Pan and W. Hu, *Small Methods*, 2025, **9**, e01279.
97 A. Edwin, T. Sulfikarali, G. Raj, A. Naniyil, R. Varghese and S. Gokulnath, *Mat. Chem. Front.*, 2025, **9**, 2794–2803.
98 C. Ma, J. Zhuang, J. Jia, B. Li, Y. He, L. Huo, N. Li and N. Zhao, *Small*, 2025, **21**, e03994.
99 S. Zeng, C. Chen, Z. Guo, C. Qin, Y. Wang, X. Liu, X. Li, H. Jeong, Y. Hao, D. Zhou, S. Long, Z. Wu, J. Wang, H. Li, X. Peng and J. Yoon, *Angew. Chem., Int. Ed.*, 2025, **64**, e202513815.
100 N. Muhammad, M. Hanif and P. Yang, *Coord. Chem. Rev.*, 2024, **499**, 215507.
101 N. Muhammad and Z. Guo, *Curr. Opin. Chem. Biol.*, 2014, **19**, 144–153.
102 A. K. Yadav, R. Kushwaha, A. A. Mandal, A. Mandal and S. Banerjee, *J. Am. Chem. Soc.*, 2025, **147**, 7161–7181.
103 S. Li, H. Yuan, X.-Z. Yang, X. Xu, W. Yu, Y. Wu, S. Yao, J. Xie, W. He, Z. Guo and Y. Chen, *ACS Cent. Sci.*, 2025, **11**, 441–451.
104 Y.-Y. Ling, Q.-H. Shen, L. Hao, Z.-Y. Li, L.-B. Yu, X.-X. Chen and C.-P. Tan, *ACS Appl. Mater. Interfaces*, 2025, **17**, 15237–15249.
105 L. Cai, H. Chen, Y. Wang, J. Zhang, D. Song, Y. Tan, Z. Guo and X. Wang, *J. Med. Chem.*, 2025, **68**, 9162–9175.
106 N. Muhammad, C.-P. Tan, K. Muhammad, J. Wang, N. Sadia, Z.-Y. Pan, L.-N. Ji and Z.-W. Mao, *Inorg. Chem. Front.*, 2020, **7**, 4010–4019.
107 D. Zhao, H. Zhen, J. Xue, Z. Tang, X. Han and Z. Chen, *J. Inorg. Biochem.*, 2024, **251**, 112437.
108 J. Yang, D.-L. Chen, P.-C. Wang, B. Yang and C.-Z. Gao, *Eur. J. Med. Chem.*, 2022, **243**, 114702.
109 S. Wu, X. Wang, Y. He, Z. Zhu, C. Zhu and Z. Guo, *J. Inorg. Biochem.*, 2014, **139**, 77–84.
110 S. Jin, Y. He, C. Feng, J. Yuan, Y. Guo, Z. Guo and X. Wang, *ACS Cent. Sci.*, 2025, **11**, 393–403.
111 H. Jin, L. Wang and R. Bernards, *Nat. Rev. Drug Discovery*, 2023, **22**, 213–234.
112 J. Liang, H. Wang, W. Ding, J. Huang, X. Zhou, H. Wang, X. Dong, G. Li, E. Chen, F. Zhou, H. Fan, J. Xia, B. Shen, D. Cai, P. Lan, H. Jiang, J. Ling, Z. Cheng, X. Liu and J. Sun, *Sci. Adv.*, 2020, **6**, eabc3646.
113 H. Singh, N. Kinarivala and S. Sharma, *Anticancer Agents Med. Chem*, 2019, **19**, 842–874.
114 A. Doostmohammadi, H. Jooya, K. Ghorbanian, S. Gohari and M. Dadashpour, *Cell Commun. Signaling*, 2024, **22**, 228.
115 S. Zhang, D. Song, W. Yu, J. Li, X. Wang, Y. Li, Z. Zhao, Q. Xue, J. Zhao, J. P. Li and Z. Guo, *Natl. Sci. Rev.*, 2024, **11**, nwae020.
116 S. Yang, J. Ma, E. He, Z. Xiong, Y. Fan, C. Ding and A. Zhang, *Chem. Eng. J.*, 2025, **511**, 162042.
117 S. Lionello, G. Marzaro and D. Martinvalet, *Pharmacol. Res.*, 2020, **160**, 105196.
118 L. Chen, J. Dong, S. Liao, S. Wang, Z. Wu, M. Zuo, B. Liu, C. Yan, Y. Chen, H. He, Q. Meng and Z. Song, *Hepatology*, 2022, **76**, 1389–1408.
119 C. Zheng, Y. Chen, T. He, Y. Xiu, X. Dong, X. Wang, X. Wen, C. Li, Q. Yao, S. Chen, X. Zhan, L. Gao and Z. Bai, *Mol. Med.*, 2024, **30**, 160.
120 R. Fan, R. Lin, S. Zhang, A. Deng, Y. Hai, J. Zhuang, Y. Liu, M. Cheng and G. Wei, *Acta Pharm. Sin. B*, 2024, **14**, 1742–1758.
121 E. J. Ge, A. I. Bush, A. Casini, P. A. Cobine, J. R. Cross, G. M. DeNicola, Q. P. Dou, K. J. Franz, V. M. Gohil, S. Gupta, S. G. Kaler, S. Lutsenko, V. Mittal, M. J. Petris, R. Polishchuk, M. Ralle, M. L. Schilsky, N. K. Tonks, L. T. Vahdat, L. Van Aelst, D. Xi, P. Yuan, D. C. Brady and C. J. Chang, *Nat. Rev. Cancer*, 2022, **22**, 102–113.
122 D. Tang, X. Chen and G. Kroemer, *Cell Res.*, 2022, **32**, 417–418.
123 L. Li, H. Zhou and C. Zhang, *Cell. Mol. Biol. Lett.*, 2024, **29**, 91.
124 K. Lu, C. S. Wijaya, Q. Yao, H. Jin and L. Feng, *Cancer Commun.*, 2025, **45**, 505–524.
125 D. Tang, G. Kroemer and R. Kang, *Nat. Rev. Clin. Oncol.*, 2024, **21**, 370–388.
126 C. Pan, Z. Ji, Q. Wang, Z. Zhang, Z. Wang, C. Li, S. Lu and P. Ge, *CNS Neurosci. Ther.*, 2024, **30**, e70039.

127 C. Zhu, J. Li, W. Sun, D. Li, Y. Wang and X.-C. Shen, *JACS Au*, 2024, **4**, 3988–3999.
128 V. A. Meshcheryakova, V. P. Grivin, A. V. Mikheylis, Y. P. Tsentalovich, A. A. Kokorenko, I. P. Pozdnyakov, K. S. Ershov, A. V. Baklanov, A. E. Zazulya, D. B. Vasilchenko, A. A. Melnikov, S. V. Chekalin and E. M. Glebov, *J. Lumin.*, 2024, **275**, 120804.
129 Y. Zheng, X.-X. Chen, D.-Y. Zhang, W.-J. Wang, K. Peng, Z.-Y. Li, Z.-W. Mao and C.-P. Tan, *Chem. Sci.*, 2023, **14**, 6890–6903.
130 M. Nafees, M. Hanif, R. Muhammad Asif Khan, F. Faiz and P. Yang, *ChemMedChem*, 2024, **19**, e202400289.
131 W. Xu, S. Zhu, Z. Sun, J. Ye and H. Chu, *Acta Pharm. Sin. B*, 2025, **16**(4), 2196–2231.
132 W. Wang, Y. Xu, Y. Tang and Q. Li, *Adv. Mater.*, 2025, **37**, 2416122.
133 Y.-Y. Ling, Z.-Y. Li, X. Mu, Y.-J. Kong, L. Hao, W.-J. Wang, Q.-H. Shen, Y.-B. Zhang and C.-P. Tan, *Eur. J. Med. Chem.*, 2024, **275**, 116638.
134 A. Ahmad, A. E. Graminha, Anam, A. Nazir, S. H. Mendes Abe, M. V. Palmeira-Mello, J. L. Dutra, W. P. D. Badaro, A. B. Lazzarini, T. R. de Moura, S. Khan, A. A. Batista, A. V. G. Netto and J. C. M. Pereira, *Polyhedron*, 2025, **282**, 117788.
135 V. N. Vadakkedathu Palakkeezhillam, J. Haribabu, K. S. Karthik, V. Suresh Kumar, V. Manakkadan, P. Rasin, M. Garg, A. Arulraj, D. Moraga and A. Sreekanth, *New J. Chem.*, 2025, **49**, 11531–11547.
136 G. Xu, Q. Liang, L. Gao, S. Xu, W. Luo, Q. Wu, J. Li, Z. Zhang, H. Liang and F. Yang, *J. Med. Chem.*, 2024, **67**, 19573–19585.
137 M. Hemagirri, Y. Chen, S. C. B. Gopinath, S. Sahreen, M. Adnan and S. Sasidharan, *Biochimie*, 2024, **221**, 159–181.
138 W. Zhang, Y. Shi, L. Oyang, S. Cui, S. Li, J. Li, L. Liu, Y. Li, M. Peng, S. Tan, L. Xia, J. Lin, X. Xu, N. Wu, Q. Peng, Y. Tang, X. Luo, Q. Liao, X. Jiang and Y. Zhou, *Cell Death Discovery*, 2024, **10**, 343.
139 S. Zhuang, Q. Li, L. Cai, C. Wang and X. Lei, *ACS Centr. Sci.*, 2017, **3**, 501–509.
140 H. G. Xu, M. Schikora, M. Sisa, S. Daum, I. Klemt, C. Janko, C. Alexiou, G. Bila, R. Bilyy, W. Gong, M. Schmitt, L. Sellner and A. Mokhir, *Angew. Chem., Int. Ed.*, 2021, **60**, 11158–11162.
141 B.-F. Liang, S. Jiang, Y.-S. Zhi, Z.-Y. Pan, X.-Q. Su, Q. Gong, Z.-D. He, D.-H. Yao, L. He and C.-Y. Li, *Inorg. Chem. Front.*, 2025, **12**, 2294–2302.
142 T. Pandey and V. Pandey, *Nitric Oxide*, 2024, **144**, 20–28.
143 T. Pandey, R. S. Kaundal and V. Pandey, *Biophy. Chem.*, 2024, **314**, 107317.
144 B. D. Paul, S. H. Snyder and K. Kashfi, *Redox Biol.*, 2021, **38**, 101772.
145 W. Gao, Y.-F. Liu, Y.-X. Zhang, Y. Wang, Y.-Q. Jin, H. Yuan, X.-Y. Liang, X.-Y. Ji, Q.-Y. Jiang and D.-D. Wu, *Cell Death Discovery*, 2024, **10**, 114.
146 J. S. Nam, M. S. Dixon and I. I. C. Chio, *Mol. Cell*, 2024, **84**, 3865–3867.
147 J. Zhang, X. Cao, H. Wen, Q. T. H. Shubhra, X. Hu, X. He and X. Cai, *Coord. Chem. Rev.*, 2025, **539**, 216746.
148 Y. Li, B. Liu, Y. Zheng, M. Hu, L.-Y. Liu, C.-R. Li, W. Zhang, Y.-X. Lai and Z.-W. Mao, *J. Med. Chem.*, 2024, **67**, 16235–16247.
149 Y. Yin, X. Cheng, D. Fan, Y. Fang, H. Li, X. Zhou, H. Guo, W. Zeng and F. Chen, *Mol. Pharm.*, 2025, **22**, 6302–6316.
150 H. Li, T. Yang, J. Zhang, K. Xue, X. Ma, B. Yu and X. Jin, *Cell Death Discovery*, 2024, **10**, 32.
151 Y. Hou, W. Li, J. Yang, H. Yu, C. Wang, Y. Li, S. Lv and L. Zhang, *Cell Death Discovery*, 2025, **16**, 568.
152 M. Bipasha, V. Deepali, D. Prabal, K. Supriya and B. Megha, *Asia-Pacific J. Clinic. Oncol.*, 2025, **21**, 465–473.
153 M. Pourhabib Mamaghani, S. N. Mousavikia and H. Azimian, *Pathol. Res. Pract.*, 2025, **269**, 155907.
154 Y.-L. Zeng, L.-Y. Liu, T.-Z. Ma, Y. Liu, B. Liu, W. Liu, Q.-H. Shen, C. Wu and Z.-W. Mao, *Angew. Chem., Int. Ed.*, 2024, **63**, e202410803.
155 H. Song, N. Montesdeoca, E. Efanova, X. Li, J. Karges, H. Xiao, K. Shang and H. Zhang, *J. Controlled Release*, 2025, **384**, 113942.
156 Y. Lu, X. Ma, X. Chang, Z. Liang, L. Lv, M. Shan, Q. Lu, Z. Wen, R. Gust and W. Liu, *Chem. Soc. Rev.*, 2022, **51**, 5518–5556.
157 M. Liu, H. Liu, Y. Yang, X. Xiong and T. Zou, *J. Am. Chem. Soc.*, 2025, **147**, 15719–15731.
158 S. M. Mahdavi, D. Bockfeld, I. V. Esarev, P. Lippmann, R. Frank, M. Brönstrup, I. Ott and M. Tamm, *RSC Med. Chem.*, 2024, **15**, 3248–3255.
159 F. Li, Z. Wen, C. Wu, Z. Yang, Z. Wang, W. Diao, D. Chen, Z. Xu, Y. Lu and W. Liu, *J. Med. Chem.*, 2024, **67**, 1982–2003.
160 C. H. Kim, E. S. Lee, H. Ko, S. Son, S. H. Kim, C. H. Lee, H.-K. Na, J. M. Shin and J. H. Park, *Chem. Mater.*, 2024, **36**, 1088–1112.
161 L. Feng, J. Sang, H. Zhu, Y. Hu, B. Liu, G. He, L. Yang, C. Yu, Y. Zhu and P. Yang, *Adv. Mater.*, 2025, **37**, e10010.
162 J. Li, X. Pang, Z. Xin, L. Song, X. Liu, X. Zhang and Z. Yang, *Mater. Today Bio*, 2025, **34**, 102133.
163 L. Liu, H. Lei, G. Hou, L. Zhang, Y. Chen, Y. Lu, Z. Pei, J. Ge, J. Wu, J. Zhou and L. Cheng, *ACS Nano*, 2024, **18**, 12830–12844.
164 S. Yao, F. Xu, Y. Wang, J. Shang, S. Li, X. Xu, Z. Liu, W. He, Z. Guo and Y. Chen, *J. Am. Chem. Soc.*, 2025, **147**, 11132–11144.
165 H. Zhao, S. Jin, Y. Liu, Q. Wang, B. S. N. Tan, S. Wang, W.-K. Han, X. Niu and Y. Zhao, *J. Am. Chem. Soc.*, 2025, **147**, 4871–4885.
166 Z. Pei, L. Li, N. Yang, S. Sun, N. Jiang and L. Cheng, *Coord. Chem. Rev.*, 2024, **517**, 215969.
167 W. Wang, F. Yang, L. Zhang, M. Wang, L. Yin, X. Dong, H. Xiao and N. Xing, *Adv. Mater.*, 2024, **36**, 2308762.
168 X. Li, J. Cai, H. Zhang, S. Sun, S. Zhao, Z. Wang, X. Nie, C. Xu, Y. Zhang and H. Xiao, *ACS Nano*, 2024, **18**, 7852–7867.

169 K. Shang, D. Tang, M. Cui, H. Hou, B. Xiao, J. Liu, R. Zhang, R. Kuai, J. Liu, H. Xiao, F. Huang and J. Wang, *Adv. Mater.*, 2025, **37**, e06011.
170 L. Liu, S. Fu, H. Gu, Y. Li, G. Zhu, H. Ai and W. Li, *ACS Nano*, 2025, **19**, 2726–2741.
171 X. Zhang, D. Tang, H. Xiao, B. Li, K. Shang and D. Zhao, *ACS Nano*, 2025, **19**, 4346–4365.
172 R. Feng, A. Chu, Y. Guo, G. Hu and B. Zhang, *Adv. Eng. Mater.*, 2025, 2402392.
173 R. Huang, N. Ni, Y. Su, L. Gu, Y. Ju, D. Zhang, J. Li, M. Chang, Y. Chen, P. Gu and X. Fan, *Chem. Eng. J.*, 2024, **479**, 147436.
174 X. Rong, S. Xiao, W. Geng, B. Zhu, P. Mou, Z. Ding, B. Zhang, Y. Fan, L. Qiu and C. Cheng, *Nat. Commun.*, 2025, **16**, 6150.
175 Z. Yan, Y. Deng, L. Huang, J. Zeng, D. Wang, Z. Tong, Q. Fan, W. Tan, J. Yan, X. Zang and S. Chen, *J. Nanobiotechnol.*, 2025, **23**, 286.
176 F. Wang, Z. Wang, S. Huang, J. Yang, Y. Chen and H. Chao, *Chem. – Eur. J.*, 2025, **31**, e202501016.
177 X.-X. Chen, Z.-Y. Li, Q.-H. Shen, K. Peng, P. Wang, L.-B. Yu, Y.-Y. Han and C.-P. Tan, *ACS Nano*, 2025, **19**, 26953–26967.
178 Z. Wang and Z. Xi, *Tetrahedron*, 2021, **87**, 132096.
179 Z. Xie, Y. Yang, D. Ma and Z. Xi, *Org. Biomol. Chem.*, 2024, **22**, 606–620.
180 G. Yi, V. P. Brendel, C. Shu, P. Li, S. Palanathan and C. Cheng Kao, *PLoS One*, 2013, **8**, e77846.
181 Z. Vavřina, O. Gutten, M. Smola, M. Zavřel, Z. Aliakbar Tehrani, V. Charvát, M. Kožíšek, E. Boura, G. Birkuš and L. Rulíšek, *Biochemistry*, 2021, **60**, 607–620.
182 M. Nafees, F. He, L. Feng, M. Hanif and P. Yang, *Inorg. Chem. Front.*, 2025, **12**, 4151–4177.
183 K. Zhao, J. Huang, Y. Zhao, S. Wang, J. Xu and K. Yin, *Biochim. Biophys. Acta Rev. Cancer*, 2023, **1878**, 188983.
184 Z. Cao, Y. Zhang, H. Jia, X. Sun, Y. Feng, H. Wu, B. Xu and Z. Wei, *Cytokine*, 2025, **187**, 156873.
185 B. K. Allen, M. M. Kulkarni, B. Chamberlain, T. Dwight, C. Koh, R. Samant, F. Jernigan, J. Rice, D. Tan, S. Li, K. Marino, H. Huang, E. Chiswick, B. Tesar, S. Sparks, Z. Lin, T. D. McGee, I. Kolossváry, C. Lin, S. Shechter, H. Soutter, C. Bastos, M. Taimi, S. Lai, A. Petrin, T. Kane, S. Swann, H. Gardner, C. Winter and W. Sherman, *bioRxiv*, 2022, 493001.